Integration of real-time traffic management and train control for rail networks
Part 2: Extensions towards energy-efficient train operations

Luan, Xiaojie; Wang, Yihui; De Schutter, Bart; Meng, Lingyun; Lodewijks, Gabriel; Corman, Francesco

DOI
10.1016/j.trb.2018.06.011

Publication date
2018

Document Version
Accepted author manuscript

Published in
Transportation Research Part B: Methodological

Citation (APA)
Luan, X., Wang, Y., De Schutter, B., Meng, L., Lodewijks, G., & Corman, F. (2018). Integration of real-time traffic management and train control for rail networks: Part 2: Extensions towards energy-efficient train operations. *Transportation Research Part B: Methodological*, *115*, 72-94. https://doi.org/10.1016/j.trb.2018.06.011

Integration of real-time traffic management and train control for rail networks - Part 2: Extensions towards energy-efficient train operations

Xiaojie Luan, Yihui Wang, Bart De Schutter, Lingyun Meng,
Gabriel Lodewijks, and Francesco Corman

Published in Transportation Research Part B: Methodological *DOI: https://doi.org/10.1016/j.trb.2018.06.011*

Integration of real-time traffic management and train control for rail networks - Part 2: Extensions towards energy-efficient train operations

Xiaojie Luan[a], Yihui Wang[b], Bart De Schutter[c], Lingyun Meng[d,*], Gabriel Lodewijks[e], Francesco Corman[f]

[a]*Section Transport Engineering and Logistics, Delft University of Technology, 2628 CD Delft, the Netherlands*
[b]*State Key Laboratory of Rail Traffic Control and Safety, Beijing Jiaotong University, Beijing 100044, China*
[c]*Delft Center for Systems and Control, Delft University of Technology, 2628 CD Delft, the Netherlands*
[d]*School of traffic and transportation, Beijing Jiaotong University, Beijing 100044, China*
[e]*School of Aviation, Faculty of Science, University of New South Wales, Sydney, Australia*
[f]*Institute for Transport Planning and Systems (IVT), ETH Zürich, Stefano-Franscini-Platz 5, 8093 Zürich, Switzerland*

Abstract

We study the integration of real-time traffic management and train control by using mixed-integer nonlinear programming (MINLP) and mixed-integer linear programming (MILP) approaches. In Part 1 of the paper, three integrated optimization problems, namely the $\mathrm{P_{NLP}}$ problem (NLP: nonlinear programming), the $\mathrm{P_{PWA}}$ problem (PWA: piecewise affine), and the $\mathrm{P_{TSPO}}$ problem (TSPO: train speed profile option), have been developed for real-time traffic management that inherently include train control. A two-level approach and a custom-designed two-step approach have been proposed to solve these optimization problems. In Part 2 of the paper, aiming at energy-efficient train operation, we extend the three proposed optimization problems by introducing energy-related formulations. We first evaluate the energy consumption of a train motion. A set of nonlinear constraints is first proposed to calculate the energy consumption, which is further reformulated as a set of linear constraints for the $\mathrm{P_{TSPO}}$ problem and approximated by using a piecewise constant function for the $\mathrm{P_{NLP}}$ and $\mathrm{P_{PWA}}$ problems. Moreover, we consider the option of regenerative braking and present linear formulations to calculate the utilization of the regenerative energy obtained through braking trains. We focus on two objectives, i.e., delay recovery and energy efficiency, through using a weighted-sum formulation and an ε-constraint formulation. With these energy-related extensions, the nature of the three optimization problems remains same to Part 1. In numerical experiments conducted based on the Dutch test case, we consider the $\mathrm{P_{NLP}}$ approach and the $\mathrm{P_{TSPO}}$ approach only and compare their performance with the inclusion of the energy-related aspects; the $\mathrm{P_{PWA}}$ approach is neglected due to its bad performance, as evaluated in Part 1. According to the experimental results, the $\mathrm{P_{TSPO}}$ approach still yields a better performance within the required computation time. The trade-off between train delay and energy consumption is investigated. The results show the possibility of reducing train delay and saving energy at the same time through managing train speed, by up to 4.0% and 5.6% respectively. In our case study, applying regenerative braking leads to a 22.9% reduction of the total energy consumption.

Keywords: Real-time traffic management, Train control, Integrated optimization, Energy efficient train operation, Regenerative braking

1. Introduction

Railway transport systems are of crucial importance for the competitiveness of national or regional economy as well as for the mobility of people and goods. To maintain the environmental advantage and

*Corresponding author
Email addresses: x.luan@tudelft.nl (Xiaojie Luan), yihui.wang@bjtu.edu.cn (Yihui Wang), B.DeSchutter@tudelft.nl (Bart De Schutter), lymeng@bjtu.edu.cn (Lingyun Meng), g.lodewijks@unsw.edu.au (Gabriel Lodewijks), francesco.corman@ivt.baug.ethz.ch (Francesco Corman)

business benefits of railway sectors, targets have been set by the International Union of Railways (UIC 2012) to reduce the carbon dioxide (CO_2) emissions and energy consumption from train operations by 50% and 30% respectively in 2030, compared to 1990. Such policies reflect an increasing concern for sustainability and energy efficiency. Consequently, energy-efficient train operation is attracting more and more attention, which is seen as the most important measure to reduce the environmental impacts and the costs used to power trains.

In railway transport systems, the energy efficiency is greatly influenced by the train operation strategy, which consists of the operational train timetables and the applied driving actions. The former relates to the real-time traffic management problem, i.e., (re-)scheduling train routes, orders, and passing times at stations, aiming at adjusting the impacted schedules from perturbations and reducing negative consequences. The latter concerns the train control problem, i.e., optimizing the sequence of driving regimes (maximum acceleration, cruising, coasting, and maximum braking) and the switching points between the regimes, with the aim of minimizing energy consumption. As discussed in Part 1 of this paper, the two problems are closely related to each other. In order to achieve energy-efficient train operation, one of the most promising options is to jointly consider the two problems, i.e., (re-)constructing a timetable in a way that not only allows different driving actions, but enables eco-driving actions (resulting in better energy performance). This comes from, e.g., avoiding unneeded accelerating and braking actions, which do not only lead to trains delays, but also unnecessary waste of energy. Another promising option is to incorporate regenerative braking, so that the energy generated by braking trains can be further utilized for accelerating trains, and then the overall energy consumption of train operations decreases. As a result, to compute the energy-efficient train trajectory and further achieve the energy efficiency of train operations, the focus on only train delay is not enough; approaches that not only include train delays but also evaluate energy consumption and consider regenerativ energy utilization are desired.

In most studies of the real-time traffic management problem, train delay is a commonly used objective, and any dynamics-related objective, such as energy consumption, cannot be directly considered, due to the disregard of train dynamics, However, the objective of energy consumption is considered only in train control studies. In Part 1 of this paper, the integration of the two problems has been addressed, and three integrated optimization approaches have been developed to consider both traffic-related properties (i.e., a set of times, orders, routes to be followed by trains) and train-related properties (i.e., speed trajectories) at the same time, focusing on only delay recovery. These integrated optimization approaches build up a good foundation and enable us to introduce energy-related formulations and to focus on delay recovery and energy efficiency at the same time.

In this part of the paper, we focus on the train control part of the integrated optimization approaches while including energy-related formulations. We first introduce the evaluation of energy consumption into the integrated optimization problems. To calculate the energy consumption, a set of linear constraints is proposed for the $\mathrm{P_{TSPO}}$ problem; for the $\mathrm{P_{NLP}}$ and $\mathrm{P_{PWA}}$ problems, the resistance function with a quadratic term of train speed is approximated with a piecewise constant function, in order to maintain the nature of these two optimization approaches. In addition, we consider the option of regenerative braking and present linear formulations to calculate the utilization of the energy obtained through regenerative braking. With the inclusion of the energy-related formulations, we consider two objectives, i.e., delay recovery and energy efficiency, by using a weighted-sum formulation and an ε-constraint formulation. We use the Dutch test case to conduct experiments, just as in Part 1. We compare the performance of the optimization approaches and investigate the trade-off between train delay and energy consumption. By our approaches, train delay and energy consumption can be reduced at the same time through managing the train speed, by up to 4.0% and 5.6% respectively. This demonstrates the benefit of the integration and shows great potential for energy efficiency of train operations. Moreover, the benefit of regenerative braking is shown. In our case study, when applying regenerative braking, up to 53.3% of the kinetic energy can be stored, and up to 46.6% of the stored energy is re-utilized for train acceleration, which further leads to a 22.9% reduction of the total energy consumption. In the experiments, the proposed optimization approaches can obtain feasible solutions (with good quality) of the train delay and energy consumption minimization problem, for a single direction along a 50 km corridor with 9 stations and 15 trains each hour within a computation time of 3 minutes.

The remainder of this paper is organized as follows. Section 2 provides a literature review on the studies

of the train control problem, which mostly focus on the minimization of energy consumption, and the studies focusing on maximizing the utilization of the energy regenerated by braking trains. In Section 3, after introducing the notations used in the mathematical formulations, we calculate the energy consumption of the train motion for accelerating trains and for overcoming resistances respectively. Then, formulations for calculating the utilization of the energy obtained by braking trains are constructed. In Section 4, the experimental results based on a real-world railway network are given for evaluating the performance of the optimization approaches, exploring the trade-off between train delay and energy consumption, and investigating the benefits of regenerative braking. Moreover, we examine the quality of the train speed trajectories obtained by the proposed integrated optimization approaches, by means of comparing them with the train speed trajectories obtained by using the detailed nonlinear train models as proposed by Wang et al. (2013), Liu and Golovitcher (2003), Khmelnitsky (2000). Finally, Section 5 ends the paper with conclusions and topics for further research.

2. Literature review

In the literature, energy efficiency is mostly ignored in the traffic management problem, but considered in the train control problem. We review the studies on determining the energy-efficient train trajectory in Section 2.1 and the studies focusing on optimizing the utilization of the regenerated energy in Section 2.2. We refer to the review paper by González-Gil et al. (2014), where a general overview of the energy efficiency related strategies and technologies are given, e.g., energy-efficient driving, regenerative braking, and energy metering.

In addition to the above two problems, another relevant topic is the interactions of traffic management and train control. As studies on that topic have been reviewed and discussed in Section 2.2 of Part 1, we do not elaborate them here. We refer to the review paper by Scheepmaker et al. (2017), where the energy-efficient train control and timetabling problems are discussed, in terms of mathematical models and solution approaches.

2.1. Energy-efficient train control: eco-driving strategy

The research on the train control problem for a single train started in the 1960s (Ichikawa 1968, Kokotovic and Singh 1972). Over the years, many approaches have been proposed to find the optimal train speed profile, aiming at minimizing the energy consumption. In the following we briefly review some fundamental theoretical work and the related work on numerical solution methods.

Fundamental theoretical work was established by Howlett (1990), Howlett and Pudney (1995), Howlett (2000), where the optimal train control strategy (involving four optimal control regimes, i.e., maximum accelerating, cruising, coasting, and maximum braking) was presented. The authors showed that an optimal driving strategy must have certain properties., i.e., the optimal speed profile consists of a power-cruise-coast-brake strategy. Howlett et al. (2009) extended this theoretical work by including steep sections. In a later work, Albrecht et al. (2013) used perturbation analysis to prove that the optimal switching points are uniquely defined for each steep section of track and deduced that the global optimal strategy is unique.

Several solution methods in the literature are based on finding optimal switching points to construct speed profiles, see Cheng et al. (1999), Khmelnitsky (2000), Liu and Golovitcher (2003). Cheng (1997) studied analytical approaches for dealing with multiple speed limits with continuous speeds. Khmelnitsky (2000) gave a comprehensive analysis of the optimal trajectory planning problem with a continually varying gradient and speed restrictions. The maximum principle was applied to obtain optimal operation regimes and their sequences. Moreover, Liu and Golovitcher (2003) developed an analytical approach that combines Pontryagin's principle and algebraic equations to obtain the optimal solution. Successful analytical approaches based on real-time computational algorithms were described by Albrecht et al. (2016a,b), Khmelnitsky (2000), Liu and Golovitcher (2003). These approaches derived accurate speed profiles by numerically solving solutions of equations of motion and calculating optimal switching points.

Some optimization approaches are also available in the literature to address the energy-efficient train control problem for a single train. Franke et al. (2002) proposed a discrete dynamic programming approach

to solve the optimal train control problem, with consideration of multiple speed restrictions, regenerative braking, and gravitational forces on slopes. Ko et al. (2004) applied a dynamic programming approach to find the optimal train trajectory. The original train control problem was transformed into a multi-stage decision process that can be solved in an acceptable time. Furthermore, a number of advanced techniques, such as ant colony optimization approaches and fuzzy and genetic algorithms, have been proposed to calculate the optimal train trajectory by, e.g., Han et al. (1999), Chang and Xu (2000), Lu (2011), Su et al. (2014). Vašak et al. (2009) used a multi-parametric quadratic programming method to optimize the train trajectory for train operations, where the nonlinear train model with quadratic resistance is approximated by using a piecewise affine function. Furthermore, Wang et al. (2013) solved the optimal trajectory problem as a mixed integer linear programming (MILP) problem by approximating the nonlinear terms with piecewise affine functions.

Some other studies focused on the train control problem for multiple trains. Lu and Feng (2011) considered the operation of two trains on a single line and optimized the trajectory of the following train considering the constraints caused by the leading train. A parallel genetic algorithm was proposed to optimize the trajectories for the leading train and the following train. A better train control solution with a lower energy consumption was found. Wang et al. (2014) considered the energy-efficient train control problem for multiple trains under fixed block signaling systems and moving block signaling systems, where the resulting nonlinear optimization problem is transformed into an MILP problem and solved by a greedy approach and a simultaneous approach. In Haahr et al. (2017), a dynamic programming approach based on a time-space graph formulation was proposed for optimizing train speed profiles with speed restrictions and passage points. Passage points were handled in a way that requires each train transfer from one block to the next block within a specified time-window. Yang et al. (2017b) developed an integrated timetable and speed profile optimization model with multi-phase speed limits to reduce the energy consumption for a metro line. These studies have more or less interactions with the traffic management problem, which is mostly addressed in a decomposed manner (see, e.g., D'Ariano et al. 2007, Albrecht et al. 2013), an iterative manner (see, e.g., Mazzarello and Ottaviani 2007, Lüthi 2009), or a non-optimized manner (see Wang and Goverde 2016). Since we have had relevant discussions in Section 2.2 of Part 1, we do not repeat these studies here. Readers could refer to Part 1 of the paper for more information.

2.2. Energy efficiency through applying regenerative braking

Regenerative braking is an energy recovery mechanism to transform train kinetic energy into electricity during train braking. This technique is recognized as an efficient way to improve energy efficiency of train operations. In the literature, two kinds of methods are commonly implemented to maximize the utilization of the regenerated energy: one is to use energy storage systems, either on-board energy storage devices or wayside energy storage devices, where the regenerated energy can be stored and further re-utilized for acceleration (Lambert et al. 2010, Ciccarelli et al. 2014); and another one is to schedule trains to coordinate the acceleration and deceleration of trains as much as possible (Yang et al. 2015).

Miyatake and Ko (2010) applied a dynamic programming approach to calculate the speed profiles for trains with on-board energy storage devices to enhance the regenerative utilization. Kampeerawat and Koseki (2017) presented a strategy for utilizing regenerated energy in an urban railway system by joint consideration of adjusting the train operating schedule and employing wayside energy storage systems.

Nasri et al. (2010) applied genetic algorithms for the train scheduling problem to enhance the utilization of the regenerated energy through adjusting the headways and reserve times. Peña-Alcaraz et al. (2012) proposed a train scheduling approach to maximize the utilization of regenerative braking energy by synchronizing the acceleration and deceleration between trains with consideration of the power supply network. Yang et al. (2013) proposed a cooperative train scheduling approach to coordinate the acceleration and deceleration between adjacent trains to maximize the overlapping time, where a genetic algorithm with binary encoding was designed to solve the resulting integer programming problem. Su et al. (2013) developed a cooperative train control method for multiple trains to minimize the actual energy consumption (i.e., the difference between the traction energy consumption and the utilized regeneration energy), considering a scenario that an accelerating train can reuse the regenerative energy from a braking train on the opposite direction. Li and Lo (2014) proposed an integrated energy-efficient train operation approach for urban rail

transit system to optimize the train schedule and speed profiles simultaneously, where the utilization of regenerative energy between trains in the substations is considered and the resulting problem is solved by a genetic algorithm. A fuzzy mathematical programming approach is proposed by Cucala et al. (2012) to jointly optimize the train schedule and the driving strategy, where the uncertainty of delays and the driver's behavioral response are considered. The resulting problem is solved by fuzzy mathematical programming and a genetic algorithm. A bi-objective nonlinear programming approach is proposed by Yang et al. (2017a) to optimize the energy-efficient train schedules and speed profiles simultaneously with consideration of regenerative braking. Chen et al. (2014) developed a two-objective integer programming approach to optimize the overlap time of the accelerating phases and the braking phases for contiguous trains, so as to increase the utilization of regenerative braking energy.

Most studies on improving the utilization of the regenerated energy focus on the method of scheduling trains to coordinate the acceleration and deceleration of trains as much as possible, in order to maximize the utilization of the regenerated energy. Therefore, train blocking times are adjusted to be aggregated, with the only aim of improving energy efficiency. However, there are no guarantees offered for the traffic-related performance measures, like train delay and travel time. Only a few studies focus on methods that use energy storage systems. In theory, the use of energy storage devices could attain a higher utilization rate of the regenerative energy, as the temporal limits on using the regenerated energy are released.

2.3. Paper contributions

Achieving energy efficiency is the main purpose of the studies on the train control problem and the studies on regenerative braking. Many approaches (e.g., analytical approaches, optimization-based approaches) have been proposed to address these problems, as reviewed in Section 2.1 and Section 2.2. Inspirations from these studies enable us to include energy consumption minimization into the integrated optimization problem, in order to make a significant contribution towards energy-efficient train operation. One of the main differences with the previous studies is that we consider the optimization of energy consumption, not just the evaluation of energy consumption. Moreover, energy consumption is formulated by using the formulation method proposed in Part 1, with respect to the nature of the integrated optimization problem. We summarize the main contributions of the current paper as follows:

- This paper introduces explicitly the issue of minimization of energy consumption into the integrated optimization problems of traffic management and train control (proposed in Part 1), which enables us to assess and optimize the economic (and environmental) performance (i.e., energy consumption, from a perspective of train operators) and the punctual performance (i.e., train delay, from a viewpoint of customers) of train operations simultaneously. Aiming at both delay recovery and energy efficiency, great potential is shown for energy efficiency of train operations.

- Two optimization approaches with either nonlinear constraints or linearized constraints are developed in Section 3.2, based on the foundations laid in Part 1. Two formulations, i.e., the weighted-sum formulation and the ε-constraint formulation, are considered for the optimization problems with the objectives of train delay and energy consumption. With the framework of the proposed optimization problems, regenerative braking and coasting can be modeled seamlessly, as discussed in Section 3.3.

- The performance of the proposed approaches is good, as a feasible solution with a good quality can be obtained efficiently (within 180 seconds), see Section 4.1. In our case study, we demonstrate the improvement in energy efficiency of train operations, as a trade-off with train delays. Despite the trade-off, it is proved that train delay and energy consumption can be reduced simultaneously through managing the train speeds, by up to 4.0% and 5.6% respectively in one of the test instances (see Section 4.2). Moreover, the benefit of regenerative braking on energy efficiency of train operations is shown in Section 4.3. The consideration of regenerative braking can provide an extra reduction in the energy consumption. In our test case, a 46.6% utilization of the regenerated energy results in a 22.9% reduction of the total energy consumption.

3. Mathematical formulations

In Section 3.1, we first describe the notations used for formulating, modelling, and optimizing the energy-related aspects. Section 3.2 discusses and formulates the energy consumption of the train motion for accelerating trains and for overcoming resistances respectively. As incorporating regenerative braking is an effective way to achieve energy efficiency, in Section 3.3, we consider the possibility of regenerative braking and provide formulations for calculating the utilization of the regenerative energy obtained by braking trains. In this paper (Part 2), we still follow the assumptions proposed in Part 1, which are recapitulated and explained in Appendix A.

3.1. Notations

Table 1 lists the sets, subscripts, input parameters, and decision variables used for formulating the train energy consumption. Note that the beginning/ending point of a block section or of a main/siding track in a station, or a point of merging/diverging of tracks on a segment, is represented by a node; a block section is described as a cell, which connects two nodes. Movement of a train on a block section is considered to be made up by an incoming phase, (accelerating or braking from a starting speed to a cruising speed), a cruising phase with the constant cruising speed, and an outgoing phase (accelerating or braking from the cruising speed to an exit speed of the block section).

Table 1. Sets, subscripts, input parameters, and decision variables

Symbol	Description
	Sets and subscripts
F	set of trains, $\|F\|$ is the number of trains
V	set of nodes, $\|V\|$ is the number of nodes
E	set of cells, i.e., block sections, $E \subseteq V \times V$, $\|E\|$ is the number of cells
K	set of regions, i.e., electric regions, $\|K\|$ is the number of regions
f	train index, $f \in F$
p, i, j, k	node index, $p, i, j, k \in V$
(i, j)	cell index, $(i, j) \in E$
κ	region index, $\kappa \in K$
E_f	set of cells that train f may use, $E_f \subseteq E$
$Y_{f,i,j}$	set of options of train speed profile vectors that train f may follow on cell (i, j), $\|Y_{f,i,j}\|$ is the number of train speed profile options (TSPOs) for train f on cell (i, j)
b	TSPO index, $b_{f,i,j} \in \{1, ..., \|Y_{f,i,j}\|\}$
E_f^{stop}	set of cells on which train f should stop, $E_f^{\text{stop}} \subseteq E_f$, $\|E_f^{\text{stop}}\|$ is the number of stops of train f
E_κ^{r}	set of cells in region κ where trains can utilize regenerative energy
	Input parameters
m_f	mass of train f
v_f^{turn}	train speed at the switching point of acceleration for train f
$L_{i,j}^{\text{cell}}$	length of cell (i, j)
$D_{f,i,j}$	planned arrival time of train f on cell (i, j), $(i, j) \in E_f^{\text{stop}}$
$\alpha_{1,f,i,j}$	maximum acceleration of train f on cell (i, j), when train speed is not larger than v_f^{turn}
$\alpha_{2,f,i,j}$	maximum acceleration of train f on cell (i, j), when train speed is larger than v_f^{turn}
$\beta_{f,i,j}$	maximum deceleration of train f on cell (i, j)
$y_{f,i,j,b}$	b^{th} train speed profile vector, $y_{f,i,j,b} \in Y_{f,i,j}$
$y_{f,i,j,b}^{\text{in}}, y_{f,i,j,b}^{\text{cru}}, y_{f,i,j,b}^{\text{out}}$	b^{th} incoming, cruising, and outgoing speed of train f on cell (i, j), train speed profile vector $y_{f,i,j,b} = \begin{bmatrix} y_{f,i,j,b}^{\text{in}} & y_{f,i,j,b}^{\text{cru}} & y_{f,i,j,b}^{\text{out}} \end{bmatrix}^\top \in Y_{f,i,j}$

Symbol	Description
$L^{\text{in}}_{f,i,j,b}$, $L^{\text{out}}_{f,i,j,b}$	distance that train f runs over on cell (i,j) in the incoming and outgoing phases in the b^{th} train speed profile vector $y_{f,i,j,b}$
$\zeta_{1,f,i,j,b}, \ldots,$ $\zeta_{6.f,i,j,b}$	logical parameters to indicate the relation of the incoming, cruising, outgoing speed, and switching speed v^{turn}_f in the b^{th} train speed profile vector $y_{f,i,j,b}$ (see Table 2 of Appendix A)
$r_{1,f,i,j}, r_{2,f,i,j},$ $r_{3,f,i,j}$	coefficients of the total resistance function for train f on cell (i,j)
$\eta_{i,j,p,k}$	recuperation coefficient for utilizing the regenerative energy between cells (i,j) and (p,k) depending on the distance between the two cells
	Decision variables
$a_{f,i,j}, d_{f,i,j}$	arrival and departure time of train f at cell (i,j)
$a^{\text{turn}}_{f,i,j}/d^{\text{turn}}_{f,i,j}$	time point that train f reaches the switching speed v^{turn}_f in the incoming/outgoing phase on cell (i,j)
$a^{\text{cru}}_{f,i,j}/d^{\text{cru}}_{f,i,j}$	time point that train f starts/ends cruising, i.e., the starting/ending time of cruising phase on cell (i,j)
$v^{\text{in}}_{f,i,j}, v^{\text{cru}}_{f,i,j},$ $v^{\text{out}}_{f,i,j}$	incoming speed, cruising speed, and outgoing speed of train f on cell (i,j)
$w_{f,i,j}$	dwell time of train f on cell (i,j)
$L^{\text{cru}}_{f,i,j}$	distance that train f runs through on cell (i,j) in the cruising phase
$\vartheta_{f,i,j,b}$	binary variables, $\vartheta_{f,i,j,b}=1$ if the corresponding train speed vector $y_{f,i,j,b}$ is used by train f on cell (i,j), and otherwise $\vartheta_{f,i,j,b}=0$
$J^{\text{acc\_in}}_{f,i,j}, J^{\text{acc\_out}}_{f,i,j}$	energy consumption for accelerating train f in the incoming and outgoing phases on cell (i,j)
$J^{\text{res\_in}}_{f,i,j}, J^{\text{res\_cru}}_{f,i,j},$ $J^{\text{res\_out}}_{f,i,j}$	energy consumption for overcoming the resistances of train f in the incoming, cruising, and outgoing phases on cell (i,j)
$J^{\text{reg\_in}}_{f,i,j}, J^{\text{reg\_out}}_{f,i,j}$	regenerative energy obtained by braking train f in the incoming and outgoing phases on cell (i,j)
$u_{f,f',i,j,p,k}$	energy generated by braking train f on cell (i,j) and further used for accelerating train f' on cell (p,k)

We model train movements over block sections, such that their timing can be determined, and the energy can be related to the accelerating, cruising, and braking actions happening in the train movements. Compared to Part 1, some variables for calculating the energy consumption and the regenerative energy utilization are newly added, e.g., $J^{\text{acc\_in}}_{f,i,j}$, $J^{\text{res\_in}}_{f,i,j}$, $J^{\text{reg\_in}}_{f,i,j}$, and $u_{f,f',i,j,p,k}$. Basically, these variables are a consequence of the interactions among the key variables for formulating the traffic and train related decisions introduced in Part 1, i.e., arrival time variables a, departure time variables d, and train speed variables v, for all trains in the network, with respect to the work formula, the Newton's second law of motion, the formulas of the uniformly accelerating and decelerating motions, and operational requirements.

Note that the maximum acceleration and deceleration depend on the traction and braking force. In the literature, researchers either consider the tractive force as a well-defined function of speed and control (Howlett 2000), or assume constant power (then tractive force is a function of speed, e.g., Howlett 2000), or assume a constant acceleration (Wang et al. 2016). As the goal of this paper (Part 2) is to include the minimization of the energy consumption into the integrated optimization problems proposed in Part 1 and to compare the integrated optimization approaches in a clear way, we still assume a piecewise constant acceleration (with a switching point v^{turn}_f) and a constant deceleration for each train category, just as in Part 1. So a train follows a uniform acceleration and deceleration motion in a given speed interval. According to the equation $q = r + m \cdot \alpha$ (where q, r, m, and α indicate the tractive force, resistance force, train mass, and train acceleration respectively), the introduction of resistance would result in a larger tractive force (compared with the case where the resistance is neglected), which further has impact on energy consumption. We consider the piecewise constant acceleration for the train motion, and resistance is taken

into account for determining this piecewise constant acceleration, i.e., ensuring that the tractive force used for accelerating trains and for overcoming resistance together is technically feasible (not greater than the maximum tractive force). As such, the speed/time/space profile, which was computed through neglecting resistance, continues to be a feasible profile, but the resulting energy consumption changes.

3.2. Optimization of energy consumption

Energy is mostly consumed for accelerating trains and for overcoming resistance in a train movement. In Section 3.2.1 and Section 3.2.2, we discuss and formulate the energy consumption in these two usages respectively. Thus, the problem of modelling train movements is that we have to relate energy consumption to resistance and train speed, resistance to train speed, and departure/arrival times (which are the optimization variables for the traffic management problem) to distance and train speed.

3.2.1. Energy used for accelerating trains

The energy consumption for accelerating a train with a mass of m from speed v_1 to speed v_2 can be calculated as $\frac{m}{2}\cdot(v_2^2-v_1^2)$, see also Appendix B. Based on the notations in Table 1 and formulations proposed in Part 1, we add the following constraints to determine the energy consumption used for accelerating trains in the incoming and outgoing phases respectively:

$$J^{\text{acc\_in}}_{f,i,j} = \max\left\{0, \frac{1}{2}\cdot m_f\cdot[(v^{\text{cru}}_{f,i,j})^2-(v^{\text{in}}_{f,i,j})^2]\right\}, \quad \forall f\in F,(i,j)\in E_f \tag{1}$$

$$J^{\text{acc\_out}}_{f,i,j} = \max\left\{0, \frac{1}{2}\cdot m_f\cdot[(v^{\text{out}}_{f,i,j})^2-(v^{\text{cru}}_{f,i,j})^2]\right\}, \quad \forall f\in F,(i,j)\in E_f. \tag{2}$$

In the cruising phase, energy is only used for maintaining a constant cruising speed, i.e., overcoming resistance; so no energy is consumed for train acceleration in the cruising phase.

Constraints (1)-(2) contain quadratic terms of the speed variables $v^{\text{in}}_{f,i,j}$, $v^{\text{cru}}_{f,i,j}$, and $v^{\text{out}}_{f,i,j}$. These quadratic terms will not affect the nature of the three optimization problems proposed in Part 1. Therefore, with the inclusion of (1)-(2), the solution approaches proposed in Section 4 of Part 1 can still be used to solve these problems.

3.2.2. Energy used for overcoming resistance

The energy used for overcoming resistance while changing the train speed from v_1 to v_2 can be formulated as $\int_{v_1}^{v_2}\frac{r(v)\cdot v}{\alpha}\cdot \mathrm{d}v$, where $r(\cdot)$ indicates the resistance force as a function of the train speed v and α indicates the train acceleration; we refer to Appendix B for the explanation of this formulation.

Regarding the resistance force $r(\cdot)$, it is typically assumed that there are two categories of resistances in the train motion, i.e., the train resistance and the line resistance. Besides the common impact factor of the infrastructure (train) characteristics, the train resistance only depends on the train driving strategy (i.e., the operating speed), and the line resistance is mostly determined by the characteristics of the rail network (track). In the studies on the train control problem (Davis 1926, Brünger and Dahlhaus 2008, Wang et al. 2013, Hansen et al. 2017), the resistance force $r(\cdot)$ is commonly expressed as a quadratic function of the speed, i.e., $r_{1,x}\cdot v^2+r_{2,x}\cdot v+r_{3,x}$, where $r_{\varrho,x}$ for $\varrho\in\{1,2,3\}$ are non-negative coefficients that depend on the train characteristics and the rail network (track) characteristics. We refer to Appendix B for the detailed formulations and explanations of this resistance force function. We assume that the tracks have piecewise constant gradients and curve radii, e.g., the slope and curve radius are constant for each cell (block section), but could be different from one cell to another. The tunnel resistance occurs in the cells inside the tunnels (even if the cell is partially inside the tunnel) and is equal to zero for the cells completely outside the tunnels. With this assumption, the coefficients $r_{\varrho,x}$ for $\varrho\in\{1,2,3\}$ are then constant for each train category on each cell; thus, they could be rewritten as $r_{\varrho,f,i,j}$ for $\varrho\in\{1,2,3\}$ for train f on cell (i,j). As a result, we could express the total resistance of train f on cell (i,j) as $r_{f,i,j}(v_{f,i,j}) = r_{1,f,i,j}\cdot v^2_{f,i,j}+r_{2,f,i,j}\cdot v_{f,i,j}+r_{3,f,i,j}$, which only depends on its running speed $v_{f,i,j}$. Note that the total resistance is a strictly increasing quadratic function of the speed.

Let us define a function $\Xi(v) = \frac{r_1}{4} \cdot v^4 + \frac{r_2}{3} \cdot v^3 + \frac{r_3}{2} \cdot v^2$, where $r(v) \cdot v$ is the derivative of function $\Xi(v)$, i.e., $[\Xi(v)]' = r(v) \cdot v$. Then, we could calculate the integral formula $\int_{v_1}^{v_2} \frac{r(v) \cdot v}{\alpha} \cdot \mathrm{d}v$ as $\frac{\Xi(v_2) - \Xi(v_1)}{\alpha}$, which computes the energy used for overcoming resistance when accelerating a train from speed v_1 to speed v_2 at a steady acceleration α. Note that the function $\Xi(v)$ should be train and block section relevant, due to the train and block section specified coefficients $r_{\varrho,f,i,j}$ for $\varrho \in \{1,2,3\}$.

By assuming the piecewise constant acceleration (with a switching point v_f^{turn}) and the constant deceleration for each train category, a train follows a uniform acceleration and deceleration motion in a given speed interval. We apply the formulation $\frac{\Xi(v_2) - \Xi(v_1)}{\alpha}$ to compute the energy used by train f on cell (i,j) for overcoming resistance in the incoming phase, meanwhile taking the piecewise constant acceleration into account; the formulation is given as follows:

$$J_{f,i,j}^{\text{res\_in}} = \begin{cases} \frac{\Xi_{f,i,j}(v_{f,i,j}^{\text{cru}}) - \Xi_{f,i,j}(v_{f,i,j}^{\text{in}})}{\alpha_{1,f,i,j}}, \text{ if } v_{f,i,j}^{\text{in}} \le v_{f,i,j}^{\text{cru}} \le v_f^{\text{turn}} \\ \frac{\Xi_{f,i,j}(v_{f,i,j}^{\text{cru}}) - \Xi_{f,i,j}(v_{f,i,j}^{\text{in}})}{\alpha_{2,f,i,j}}, \text{ if } v_f^{\text{turn}} \le v_{f,i,j}^{\text{in}} < v_{f,i,j}^{\text{cru}} \\ \frac{\Xi_{f,i,j}(v_f^{\text{turn}}) - \Xi_{f,i,j}(v_{f,i,j}^{\text{in}})}{\alpha_{1,f,i,j}} + \frac{\Xi_{f,i,j}(v_{f,i,j}^{\text{cru}}) - \Xi_{f,i,j}(v_f^{\text{turn}})}{\alpha_{2,f,i,j}}, \text{ if } v_{f,i,j}^{\text{in}} < v_f^{\text{turn}} < v_{f,i,j}^{\text{cru}} \\ 0, \text{ if } v_{f,i,j}^{\text{in}} > v_{f,i,j}^{\text{cru}} \end{cases} \quad \forall f \in F, (i,j) \in E_f. \tag{3}$$

A formulation similar to (3) can also be constructed for calculating the energy consumption $J_{f,i,j}^{\text{res\_out}}$ in the outgoing phase. For the sake of compactness, we do not report those details here.

In the cruising phase, a train follows a uniform motion at a certain cruising speed; so the resistance force does not change and can be easily computed by $r_{f,i,j}(v_{f,i,j}^{\text{cru}})$. Therefore, based on the work formula $J = r \cdot x$ (where J, r, and x indicate the work, force, and distance that a train travelled respectively), we can formulate the energy used by train f on cell (i,j) in the cruising phase as follows:

$$J_{f,i,j}^{\text{res\_cru}} = r_{f,i,j}(v_{f,i,j}^{\text{cru}}) \cdot L_{f,i,j}^{\text{cru}} = (r_{1,f,i,j} \cdot {v_{f,i,j}^{\text{cru}}}^2 + r_{2,f,i,j} \cdot v_{f,i,j}^{\text{cru}} + r_{3,f,i,j}) \cdot L_{f,i,j}^{\text{cru}}, \quad \forall f \in F, (i,j) \in E_f. \tag{4}$$

Constraints (3)-(4) contain either a quartic term of the train speed or a product term of the speed and distance. The inclusion of these two equations changes the nature of the P_{NLP} problem and the P_{PWA} problem and leads to difficulties in solving these two problem (i.e., the resulting problems are not able to be solved directly). However, as a set $Y_{f,i,j}$ of train speed profile options (TSPOs) is pre-defined in a preprocessing step for the P_{TSPO} problem, that problem is still an MILP problem.

To address the difficulties in solving the P_{NLP} problem and the P_{PWA} problem, we can approximate the resistance function $r_{f,i,j}(\cdot)$ by using a piecewise constant function with 2 affine parts and with constant values $r_{1,f,i,j}^{\text{cs}}$ and $r_{2,f,i,j}^{\text{cs}}$. The resulting formulations for the P_{NLP} problem and the P_{PWA} problem are presented in Appendix B. Moreover, in order to help readers understand the unchanged nature of the P_{TSPO} problem, we also reformulate (3) and (4) for the P_{TSPO} problem in Appendix B.

We consider two objectives: one is for delay recovery, just as in Part 1, i.e., reducing the sum over all trains of the mean absolute delay time at all visited stations:

$$Z^{\text{delay}} = \sum_{f \in F} \sum_{(i,j) \in E_f^{\text{stop}}} \frac{|d_{f,i,j} - w_{f,i,j} - D_{f,i,j}|}{\left|E_f^{\text{stop}}\right|}, \tag{5}$$

and another one is to achieve energy efficiency, i.e., reducing the total energy consumption for both accelerating trains and overcoming resistance:

$$Z^{\text{energy}} = \sum_{f \in F} \sum_{(i,j) \in E_f} \left(J_{f,i,j}^{\text{acc\_in}} + J_{f,i,j}^{\text{acc\_out}} + J_{f,i,j}^{\text{res\_in}} + J_{f,i,j}^{\text{res\_cru}} + J_{f,i,j}^{\text{res\_out}}\right), \tag{6}$$

where $J_{f,i,j}^{\text{acc\_in}}$ and $J_{f,i,j}^{\text{acc\_out}}$ are computed in (1)-(2), and $J_{f,i,j}^{\text{res\_in}}$, $J_{f,i,j}^{\text{res\_cru}}$, and $J_{f,i,j}^{\text{res\_out}}$ are calculated by using (20)-(21) for the P_{TSPO} problem and by following (22)-(23) for the other two problems.

For multi-objective optimization problems, the weighted-sum formulation and the ε-constraint formulation are commonly used. Therefore, aiming at both delay recovery and energy efficiency, we use the following two ways:

1) One way is to minimize the weighted sum of the two objectives. Then, the overall objective function can

be presented as

$$\min Z = \iota^{\text{delay}} \cdot Z^{\text{delay}} + \iota^{\text{energy}} \cdot Z^{\text{energy}}, \tag{7}$$

where the weights ι^{delay} and ι^{energy} are used to balance their importance, and for normalization as well.

2) Another way is to minimize the energy consumption with respect to a given upper bound $Z^{\text{delay\_ub}}$ of the train delay, formulated as

$$\min Z^{\text{energy}} \tag{8a}$$

$$\text{s.t.} \quad Z^{\text{delay}} \leq Z^{\text{delay\_ub}}. \tag{8b}$$

Additionally, in this paper (Part 2), the constraints proposed in Part 1 for the three proposed optimization problems should also be included.

3.3. Utilization of regenerated energy

An option for further improving the energy efficiency of train operations is to incorporate regenerative braking, where the kinetic energy of a running train can be converted into electrical energy when the train brakes. This electrical energy can be fed back to the catenary system for immediately accelerating other trains or stored in energy storage devices (e.g., batteries, super-capacitors, and flywheels) for train acceleration when required. Regenerative braking is a mature technology. In practice, it has been used in urban rail transit systems and also in railway transportation systems (UIC 2002). The use of regenerative braking decreases the overall energy consumption of the train motion and changes the optimal solution to the energy-efficient train control (operation) problem. Therefore, in this section, we present formulations to calculate the regenerative energy and to determine the utilization of the regenerative energy, for railway and metro systems that are equipped with this technology.

Aiming at maximizing the use of the regenerative energy and to minimizing the need of on-board resistors (which are used for dissipating the regenerative energy that cannot be used within the system), energy storage technologies have been well studied in the literature (see the review papers by Khaligh and Li (2010), González-Gil et al. (2013)) and applied in the railway industry (see the recent review paper by Ghaviha et al. 2017). Therefore, we consider the use of energy storage systems, and then the regenerative energy can be used for train acceleration when it is required. Energy storage systems can by divided into two types, i.e., the on-board energy storage systems and the wayside (or stationary) energy storage systems, which result in different rules for utilizing the regenerative energy, explained as follows:

- For the on-board energy storage systems, i.e., the storage devices are installed on the trains, a train is able to temporarily store its own braking energy and re-utilize it in the next acceleration stages. So, the energy generated by braking a train on a block section can only be further used by the train itself. This kind of system is operated in some countries, e.g., Portugal (a light rail network in the south of Lisbon (Meinert 2009)) and Germany (light rail networks in Mannheim (Steiner et al. 2007)).

- For the wayside (or stationary) energy storage systems, where the storage devices are installed along the track, the surplus regenerated energy could be absorbed and delivered when it is required for other train acceleration in the same electric region. So, the energy generated by braking a train on a block section can be further used by other trains on the block sections that are in the same electric region as the block section where the the energy is generated. In practice, this kind of system is commonly used in urban rail transit systems, e.g., metro systems in France (Boizumeau et al. 2011), Germany, China, and Spain (Siemens 2011), and also used or tested for railway transport systems in some countries, e.g., Spain (Garcia-Tabares et al. 2011) and Japan (Shimada et al. 2010, Ogasa 2010).

The installation of the on-board energy storage devices will greatly increase the train mass and will require a large space, so it is sometimes used for light rail vehicles and seldom used for railway trains. In comparison, the wayside energy storage systems have less weight and little influence on operation and maintenance (Su et al. 2016). Therefore, we consider the wayside energy storage systems to illustrate the construction of the formulations. Some modifications could be made in the following proposed formulations, in order to be

make them suited for a case with the on-board energy storage system. We discuss these modifications at the end of this section (before the remark of train coasting).

Regenerative energy is the energy converted from kinetic energy into electrical energy while braking. According to the definition of regenerative energy (Scheepmaker and Goverde 2016), we formulate the energy regenerated by the braking of the train as follows:

$$J_{f,i,j}^{\text{reg\_in}} = -\min\left\{0, \frac{1}{2}\cdot m_f \cdot [(v_{f,i,j}^{\text{cru}})^2 - (v_{f,i,j}^{\text{in}})^2]\right\}, \quad \forall f \in F, (i,j) \in E_f, \tag{9}$$

$$J_{f,i,j}^{\text{reg\_out}} = -\min\left\{0, \frac{1}{2}\cdot m_f \cdot [(v_{f,i,j}^{\text{out}})^2 - (v_{f,i,j}^{\text{cru}})^2]\right\}, \quad \forall f \in F, (i,j) \in E_f \tag{10}$$

i.e., the reduction of the train kinetic energy while braking for the incoming and outgoing phases respectively. Note that implicitly $J_{f,i,j}^{\text{acc\_in}} \cdot J_{f,i,j}^{\text{reg\_in}} = 0$ and $J_{f,i,j}^{\text{acc\_out}} \cdot J_{f,i,j}^{\text{reg\_out}} = 0$, as a train cannot accelerate and decelerate at the same time.

As discussed, the final energy consumption is not just the difference between the energy used for powering trains and the energy generated by braking trains. We need to consider the rules with regards to the temporal and spatial limitations for utilizing the regenerative energy that result from the installation position of the energy storage systems, as well as the efficiency of the regenerative braking system.

We introduce a non-negative variable $u_{f,f',i,j,p,k}$ that indicates the amount of the energy generated by braking train f on cell (i,j) and then used for accelerating train f' on cell (p,k); moreover, we let $\eta_{i,j,p,k} \in [0,1]$ be the recuperation coefficient, which determines the efficiency of the regenerative braking system between cells (i,j) and (p,k), based on the distance between the two cells.

From a temporal perspective, we ensure that the regenerative energy is available when it is used for powering trains. Therefore, the following constraints is added:

$$u_{f,f',i,j,p,k} \leq 0, \quad \text{if } a_{f,i,j} > a_{f',p,k}, \quad \forall f \in F, f' \in F, (i,j) \in E_f, (p,k) \in E_{f'} \tag{11}$$

for guaranteeing that the energy generated by train f on cell (i,j) cannot be used by train f' on cell (p,k), if train f arrives at cell (i,j) after the arrival of train f' at cell (p,k). Constraint (11) is an if-then constraint, which can be rewritten as a mixed-integer linear constraint by applying the transformation properties in Bemporad and Morari (1999).

Regarding the spatial limitations, we enforce that the energy generated by braking a train can only be used by accelerating the trains located in the same electric region. Without loss of generality, we select $|K|$ regions in the network, where each region corresponds to an electric region. We then assume that the available energy regenerated in a cell can be used by any trains traveling in the region that the cell belongs to. We denote the sets of cells in the regions as $E_1^{\text{r}}, E_2^{\text{r}}, ..., E_{|K|}^{\text{r}}$. We use the following constraint

$$\sum_{f\in F, f'\in F} u_{f,f',i,j,p,k} \leq 0, \quad \forall (i,j) \in E_f, (p,k) \in E_{f'}, \{(i,j),(p,k)\} \not\subset E_\kappa^{\text{r}}, \kappa \in K \tag{12}$$

to ensure that the regenerative energy on cell (i,j) (or (p,k)) cannot be utilized by any train on cell (p,k) (or (i,j)), if the set of the two cells $\{(i,j),(p,k)\}$ is not a subset of set E_κ^{r}, for any $\kappa \in K$, i.e., cells (p,k) and (i,j) are not in the same electric region.

To balance the generation and utilization of the regenerative energy, we have the following constraint

$$\sum_{f'\in F,(p,k)\in E_{f'}} \frac{u_{f,f',i,j,p,k}}{\eta_{i,j,p,k}} \leq (J_{f,i,j}^{\text{reg\_in}} + J_{f,i,j}^{\text{reg\_out}}), \quad \forall f \in F, (i,j) \in E_f, \tag{13}$$

for ensuring that the total usage of the regenerative energy obtained by braking train f on cell (i,j) and further used for accelerating all trains $f' \in F$ on all cells $(p,k) \in E_{f'}$ cannot exceed the available amount of the energy generated by braking train f on cell (i,j). By taking the efficiency of the regenerative braking system into account, we divide the total usage of the regenerative energy by the non-negative recuperation coefficient $\eta_{i,j,p,k}$, as presented on the left-hand side of (13). Recall that the coefficient $\eta_{i,j,p,k}$ is given based on the distance between the two cells (i,j) and (p,k).

The amount of the regenerative energy that is further utilized for accelerating trains can be determined

by

$$Z^{\text{energy\_reg}} = \sum_{f\in F}\sum_{(i,j)\in E_f}\sum_{f'\in F}\sum_{(p,k)\in E_{f'}} u_{f,f',i,j,p,k}. \tag{14}$$

The final energy consumption is then calculated as follows:

$$Z^{\text{energy\_final}} = Z^{\text{energy}} - Z^{\text{energy\_reg}}. \tag{15}$$

The term Z^{energy} is computed by using (6), including the energy used for train acceleration and for overcoming resistance. We can still use the weighted sum formulation and the ε-constraint formulation, i.e., minimizing the weighted sum of the train delays and the final energy consumption, as presented in (7) through replacing Z^{energy} by $Z^{\text{energy\_final}}$, and only minimizing the final energy consumption in (15) with respect to (8b).

We now discuss the modifications for calculating the regenerative energy in use of the on-board energy storage system. For implementing the utilization rule, i.e., the regenerative energy can only by utilized by the same train that generates it through braking, two equivalent ways can be used. The first way consists in simply requiring $\sum_{f\in F, f'\in F: f\neq f'} u_{f,f',i,j,p,k} = 0$ for preventing the regenerative energy utilization between two different trains. Alternatively, we could re-define the variable $u_{f,f',i,j,p,k}$ as $u_{f,i,j,p,k}$ for all $f \in F$, $(i,j) \in E_f$, and $(p,k) \in E_f$. Then, in (11), (13), and (14), we remove the condition term $f' \in F$ and replace $(p,k) \in E_{f'}$ by $(p,k) \in E_f$. No matter which way is used, a common change in this case is to remove (12), as the spatial limitation is not active. The first way is applicable to both the wayside and on-board energy storage systems, and it is easier for switching or integrating the two types of energy storage systems, at the expense of a larger complexity of the optimization problem. In the case with only the on-board energy storage system, using the second way is a better choice.

Remark (Coasting phase)**.** Coasting phase can be included into the proposed optimization problem by assuming a piecewise constant deceleration that depends on the cruising speed. In other words, we could consider a piecewise constant train deceleration; then, the formulation approach stays similar to the approach that includes the piecewise constant train acceleration. As a similar formulation approach can be followed, we do not present the formulations for train coasting in this paper.

Moreover, we can use the arrival and departure times of a train along its route in the solutions (which have no coasting phase) obtained by applying our integrated optimization methods to further generate an accurate train speed profile option by using train trajectory optimization approaches with the aim of minimizing the energy consumption.

4. Numerical experiments

We consider the same Dutch railway network and the same 15 trains as in Part 1; we refer to Section 5.1 of Part 1 for the description of the test case. Also same to Part 1, each train is given a randomly generated primary delay time c_f^{pri} at its origin, and we consider 10 delay cases of the primary delays following a 3-parameter Weibull distribution. Additionally, we consider 6 electric regions, corresponding to 6 station areas, as depicted in Fig. 1.

As this paper (Part 2) focuses on the energy-related extensions based on the integrated optimization approaches proposed in Part 1, the complexity of the optimization problems increases with the inclusion of energy consumption and regenerative braking. Due to the worst performance of the P_{PWA} approach evaluated in Section 5.2 of Part 1, we cannot expect this approach to perform better on the extended optimization problems. Therefore, in the experiments of Part 2, we neglect the P_{PWA} approach and only test the other two approaches, i.e., the P_{NLP} approach and the P_{TSPO} approach.

In Section 4.1, we compare the results of the P_{NLP} approach and the P_{TSPO} approach, aiming at both delay recovery and energy efficiency. Section 4.2 explores the trade-off between train delay and energy consumption, where the possibility of reducing train delay and energy consumption at the same time is shown. Both the weighted-sum formulation and the ε-constraint formulation are used for representing the two-objective optimization problem of delay recovery and energy efficiency. We further show the benefits of regenerative braking by investigating its impact on the energy consumption in Section 4.3. In order

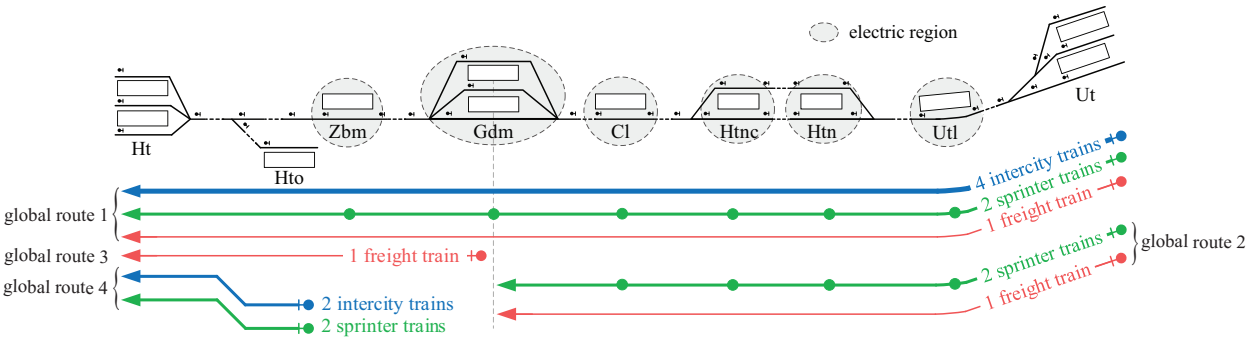

Figure 1. Part of the Dutch railway network, with 6 electric regions

to examine the solution quality of the proposed optimization approach from a train control perspective, Section 4.4 compares the train speed profiles obtained by the proposed integrated optimization approach with those obtained by using the detailed nonlinear train model as proposed by Wang et al. (2013), Liu and Golovitcher (2003), Khmelnitsky (2000). In addition to the constraints caused by the speed limits, maximum acceleration, maximum deceleration, etc., the traffic management problem also presents many operational constraints (i.e., a train should pass a certain place at a certain time, the passing time at a non-stopping station), which should be also considered in the train control problem (Wang et al. 2012). Here we apply a sequential quadratic programming (SQP) approach to solve the resulting nonlinear train control problem. The details for the solution approach will be introduced in Section 4.4. Note that the solution approaches proposed in Section 4 of Part 1 are still used to solve the $\mathrm{P_{NLP}}$ problem and the $\mathrm{P_{TSPO}}$ problem. Moreover, we additionally report the detailed data about the solutions of this test case in the online repository (Research Collection ETH Zurich).

We use the SNOPT solver implemented in the MATLAB (R2016a) TOMLAB toolbox to solve the MINLP problem, i.e., the $\mathrm{P_{NLP}}$ problem. We adopt the IBM ILOG CPLEX optimization studio version 12.6.3 with default settings to solve the MILP problem, i.e., the $\mathrm{P_{TSPO}}$ problem. The following experiments are all performed on a computer with an Intel® Core™ i7 @ 2.00 GHz processor and 16GB RAM.

4.1. Overall performance of the $\mathrm{P_{NLP}}$ *and* $\mathrm{P_{TSPO}}$ *optimization problems*

In this section, the overall performance of the $\mathrm{P_{NLP}}$ and $\mathrm{P_{TSPO}}$ optimization problems are compared; the results of the weighted-sum formulation and the ε-constraint formulation are presented in Fig. 2 and Fig. 3 respectively. For the $\mathrm{P_{TSPO}}$ optimization problem, the largest set of TSPOs (i.e., Set_1) is considered, which is generated by using the discrete speed values $\{0, 40, 60, 80, 90, 100, 110, 120, 130\}$ (km/h) for intercity and sprinter trains and $\{0, 20, 30, 40, 50, 60, 70, 80\}$ (km/h) for freight trains, as its solution quality is the best among the six sets, discussed in Section 5.4, Part 1 of the paper. This set contains 16402 speed profiles per train per block section, which results in 5.70×10^{50} possibilities of combining the speed profiles for all train services. For the weighted-sum formulation, we use 10 weights (in the form of $[\iota^{\mathrm{delay}}, \iota^{\mathrm{energy}}]$, widely ranged, see the X-axis of Fig. 2) to balance their importance, and for normalization as well. As the weight of energy consumption ι^{energy} is always set to be 1, we can also use a single weight, denoted as $\iota = \iota^{\mathrm{delay}}$, to describe the multiple choices of weights. An increase of the single weight ι implies that the importance of the train delay increases. For the ε-constraint formulation, we consider 5 upper bounds for the train delay, which stem from the delay time in the initial solution and in the secondary solutions within 180, 300, 600, and 3600 seconds of computation time (refer to Section 5.4 of Part 1), indicated as $I^{\mathrm{delay}}_{\mathrm{initial}}$, I^{delay}_{180}, I^{delay}_{300}, I^{delay}_{600}, and $I^{\mathrm{delay}}_{3600}$ respectively. We consider two computation time limits, i.e., 180 seconds and 3600 seconds, in the case of using the weighted-sum formulation. When using the ε-constraint formulation, the solution is almost never improved after 600 seconds; so we consider 600 seconds as the maximum computation time limit, instead of 3600 seconds.

In Fig. 2 and Fig. 3, each bar indicates an average result of 10 delay cases. In the upper portion of each figure, the objective values are given, indicated as gray bars for the $\mathrm{P_{NLP}}$ problem and as black bars for

the P_{TSPO} problem; in the lower portion of each figure, each white bar indicates the average improvement, i.e., $\frac{P_{NLP}\text{ solution}-P_{TSPO}\text{ solution}}{P_{NLP}\text{ solution}} \times 100\%$. A positive value means that the P_{TSPO} solution is better; a negative value implies a better solution quality of the P_{NLP} problem. Note that, in Fig. 2, we present the objective values, i.e., the real values of the train delay and the energy consumption multiplied by the weights, as we aim at comparing the overall performance of the two approaches; in all other remaining representations of the results (i.e., in Fig. 3-Fig. 10), we always present the real values of the delay time and the energy consumption.

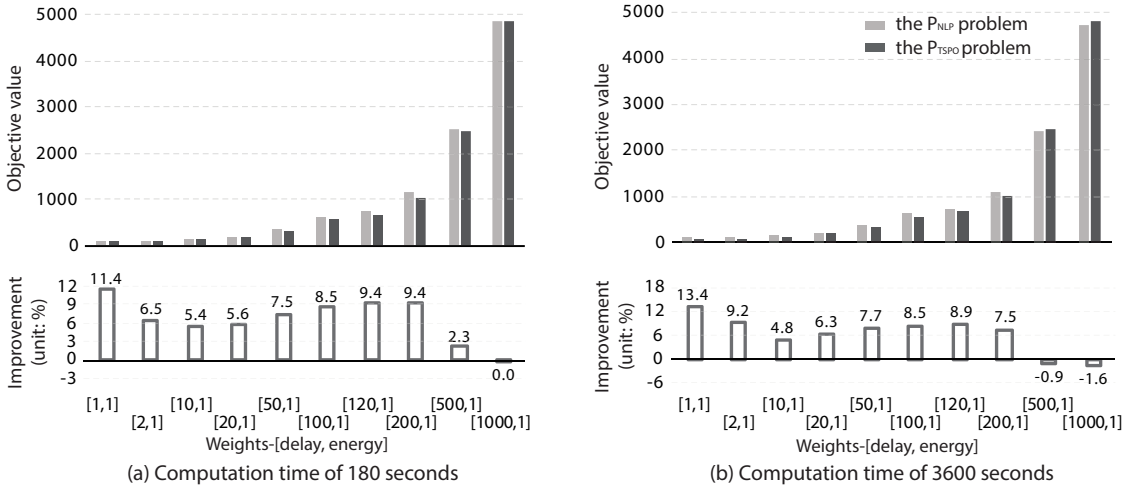

Figure 2. Comparison of the P_{NLP} and P_{TSPO} results, in the case of using the weighted-sum formulation

As illustrated in Fig. 2, the P_{TSPO} problem obtains better solutions in almost all instances, achieving 13.4% improvement in the objective value at most. When the train delay is considered very important, the P_{NLP} solution has a quality that is similar to that of the P_{TSPO} solution within 180 seconds of computation time in Fig. 2(a); with a larger computation time of 3600 seconds in Fig. 2(b), the P_{NLP} solution is about 1.6% better than the P_{TSPO} solution. From the viewpoints of both solution quality and computational efficiency, we conclude that the P_{TSPO} problem performs better in the case of using the weighted-sum formulation.

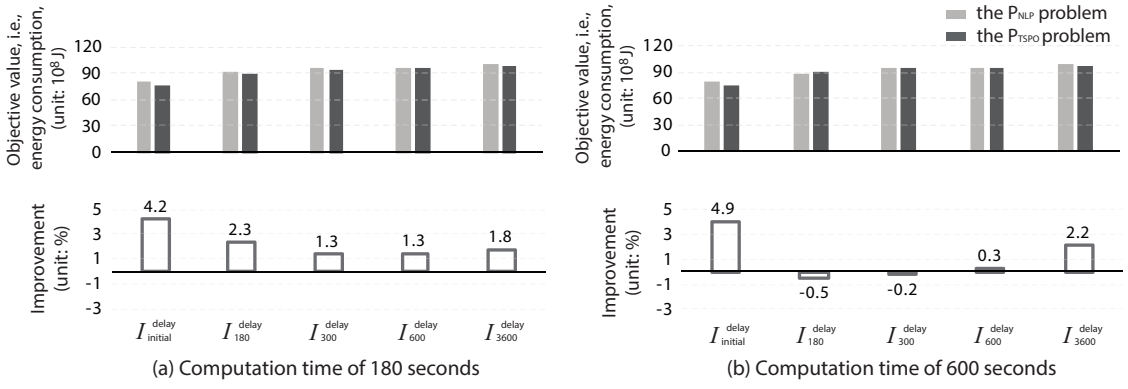

Figure 3. Comparison of the P_{NLP} and P_{TSPO} results, in the case of using the ε-constraint formulation

The results of the two optimization problems by using the ε-constraint formulation are comparatively given in Fig. 3, which has the same structure as Fig. 2. When considering the ε-constraint formulation, the performance of the two optimization problems is similar to their performance in the case of using the

weighted-sum formulation, but the difference of the two problems in solution quality is smaller. In most instances, the P_{TSPO} problem still has a better performance, achieving up to 4.2% improvement in the energy consumption. In a few other instances with 600 seconds of computation time, the P_{NLP} problem performs better, but it has only a small (less than 0.5%) improvement in the energy consumption. Overall, the P_{TSPO} optimization approach is recognized for having a better performance, by using either the ε-constraint formulation or the weighted-sum formulation.

4.2. Exploration of the trade-off between train delay and energy consumption

Due to the good performance of the P_{TSPO} approach evaluated in Section 4.1, we apply this approach to investigate the trade-off between train delay and energy consumption in this section. We present the results of the weighted-sum formulation in Section 4.2.1. The results of the ε-constraint formulation are analyzed in Section 4.2.2.

4.2.1. The weighted-sum formulation: minimization of both train delay and energy consumption

Fig. 4(a) and Fig. 4(b) illustrate the deviations of train delay and energy consumption respectively from the initial solution[1], within 180 and 3600 seconds of computation time. The red vertical line (zero line) is the benchmark, representing the initial solution. Each bar indicates an average result of ten delay cases. The gray dashed box in Fig. 4(a) is a zoom-in, using the interval $[-0.02, 1.00]$ $\times 10^3$ of the X-axis. The Y-axis represents the weights considered. From the bottom to the top of the Y-axis, the importance of the train delay increases. It should be noted that a negative value in Fig. 4 indicates a reduction (an improvement) from the initial solution, and a positive value means an increase.

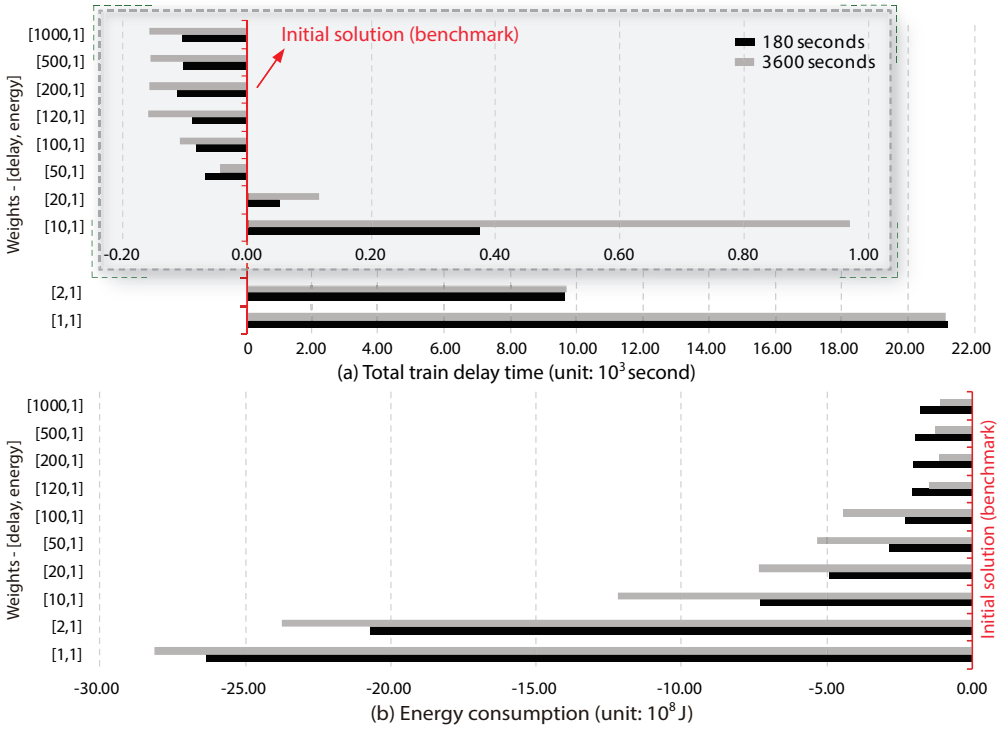

Figure 4. Deviations of train delay and energy consumption with respect to the initial solution

[1]The initial solution is obtained by considering a fixed full TSPO (train speed profile option) for each train on each block section, which is further improved to generate secondary solutions by considering a larger set of multiple TSPOs. We refer to Section 4 of Part 1 for more details.

As shown, compared with the initial solution, the energy consumption is reduced with a decreasing weight ι, while the total train delay time increases. When the weight ι is not larger than 20, the energy consumption is significantly reduced, at the expense of larger train delay times (corresponding to the positive values in Fig. 4(a)). In such cases, trains are required to run slowly for saving energy, and train delay is not the determining factor. When the weight ι is not less than 50, the train delay and energy consumption are both reduced with respect to the initial solution. The reduction of the energy consumption becomes smaller with an increasing weight ι, while the reduction of the train delay becomes larger. *The possibility of reducing train delays and saving energy at once by managing train speed is evident, achieving up to a 4.0% and 5.6% reduction of train delay and energy consumption respectively, demonstrating the benefits of the integration of traffic management and train control again.* Moreover, the extension of the computation time to 3600 seconds improves the solution quality, but the improvement is not as significant as that at 180 seconds for most cases.

4.2.2. The ε-constraint formulation: energy-saving with respect to an upper bound for train delay

In Fig. 5, we respectively present the train delay and the energy consumption, obtained by using the ε-constraint formulation (i.e., minimizing the energy consumption with respect to the given upper bound of the train delay), as a function of the computation time. We consider 5 upper bounds for the train delay, indicated as $I^{\text{delay}}_{\text{initial}}$, I^{delay}_{180}, I^{delay}_{300}, I^{delay}_{600}, and I^{delay}_{3600} respectively. We distinguish them by using colors in Fig. 5. The lighter the color becomes, the stricter the upper bound for the train delay required is, i.e., the requirement of the train delay becomes stricter in a sequence of $I^{\text{delay}}_{\text{initial}}$, ..., I^{delay}_{3600}.

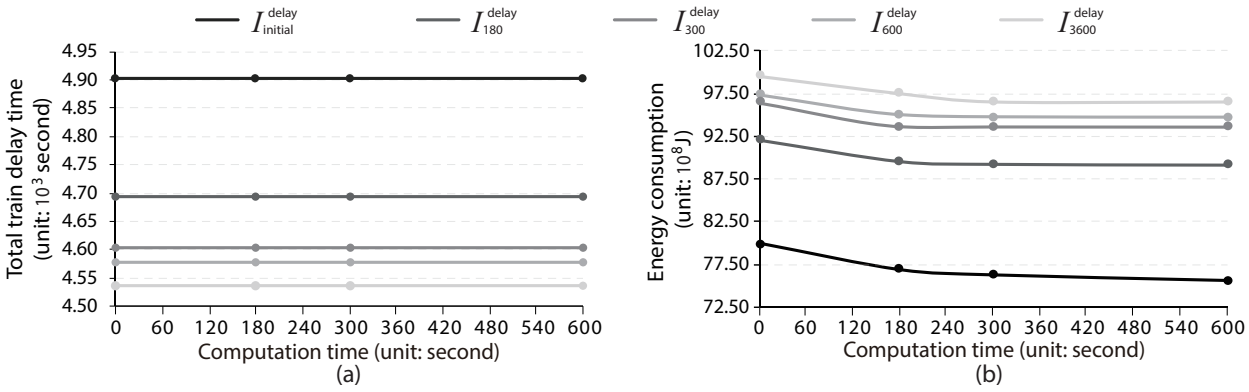

Figure 5. Evolution of the train delay and the energy consumption as a function of the computation time

In all cases, a reduction of energy consumption can be always achieved within the first 180 seconds of computation time; however, the energy consumption is almost not reduced anymore after 300 seconds. Since the train delay is considered as a hard constraint, there is little room for its improvement, i.e., the lines of the delay time in Fig. 5(a) are almost flat. Moreover, the trade-off between the train delay and the energy consumption is clearly shown in Fig. 5. A stricter upper bound of the train delay leads to less delays (i.e., the lighter line is lower in Fig. 5(a)), more energy consumption (i.e., the lighter line is higher than the darker line in Fig. 5(b)), and less saved energy (i.e., the gradient of the darker line is larger than that of the lighter line in Fig. 5(b)).

Overall, the two formulation methods both perform well. However, the ε-constraint formulation requires an appropriate upper bound for the train delay, which is generally hard to determine. On one hand, a tighter upper bound for train delay will lead to a worse performance on the energy consumption, which is reflected in the increase of the energy consumption in Fig. 5(b), and it may even result in infeasibility of the optimization problem. On the other hand, if we use a looser upper bound, the train delay could be large, even if there is some room for its reduction; therefore, the performance of the train dispatching problem cannot be guaranteed. Moreover, we find solutions where the train delay and the energy consumption are reduced at the same time from the initial solution by using the weighted-sum formulation; however, in the

solutions of the ε-constraint formulation, we can only see the reduction of the energy consumption, but no improvement in the train delay. Based on the above reasons, we conclude that the weighted-sum formulation is better and more applicable than the ε-constraint formulation.

4.3. Benefits of regenerative braking

This section compares the results with and without regenerative braking. The composition of the energy consumption in the solutions obtained based on the Dutch test case is illustrated in Fig. 6. The Y-axis represents the weights considered. From the top to the bottom of the Y-axis, the importance of the train delay increases. The X-axis represents the energy consumption. For each weight, an average result of 10 delay cases is provided. Each black (vertical) bar indicates the total energy consumption without regenerative braking. The light gray and dark gray areas indicate 80% and 60% of this total energy consumption respectively, given as benchmarks. Each dark blue bar indicates the energy used for overcoming resistance in acceleration and cruising. As a result, the difference between the total energy consumption and the energy consumed for overcoming resistance in acceleration and cruising is in fact the energy used for train acceleration, which is converted into the train kinetic energy, indicated by a light blue line. A small part of this train kinetic energy is further consumed for overcoming resistance in deceleration, represented by a light blue bar. By applying regenerative braking, some of this kinetic energy can be stored in energy storage devices, and we use a light green bar to indicate the energy stored during train braking. Then, a part of the energy stored is further re-utilized for train acceleration, which results in a reduction of the total energy consumption from the black bar to the black circle, i.e., the difference between the black bar and the black circle indicates the energy re-utilized. The energy loss of the regenerated energy due to system efficiency (i.e., caused by the recuperation coefficient η) is represented by a bar with green border.

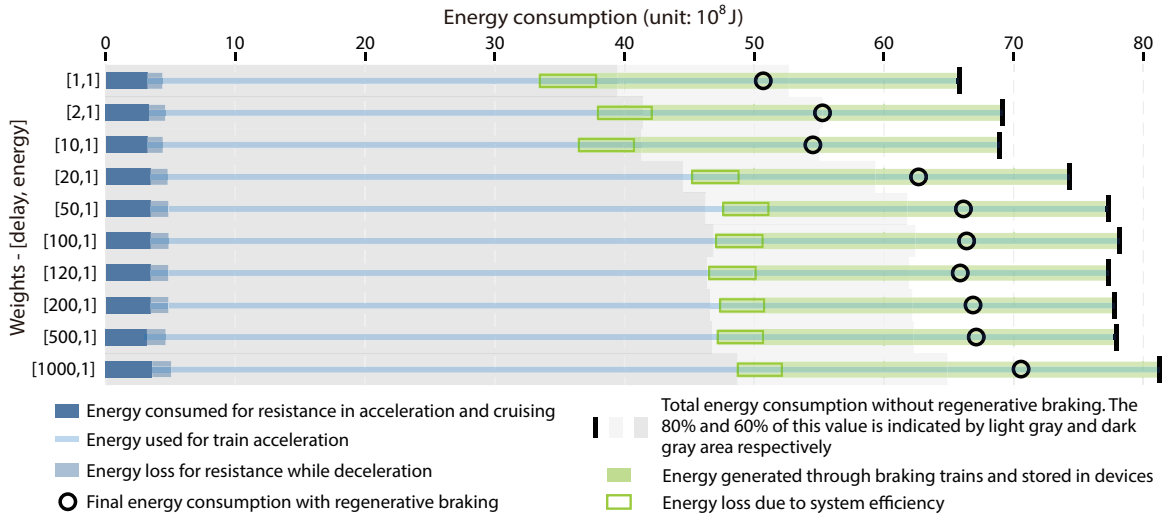

Figure 6. Composition of the energy consumption

As illustrated in Fig. 6, the total energy consumption decreases with the increase of the importance of the energy consumption. The percentage of the energy re-utilized is larger when considering the energy consumption to be more important. Moreover, in our solutions, there is a large amount (around 40%-50%) of the train kinetic energy that is not stored, indicated by the difference of the lengths between the light blue line and the light green bar. One reason for this unstored energy is due to the configuration of the electric regions, i.e., the Den Bosch (Ht) station area is not considered as an electric region of regenerative braking, so that regenerative braking cannot be applied in this station area, as shown in Fig. 1. Another reason is that the Den Bosch (Ht) station is the destination for most trains, so that many train braking actions happen in this area. As regenerative braking cannot be used in the Den Bosch (Ht) station, the train kinetic energy in these braking actions is all lost. In fact, the composition of the energy consumption strongly

depends on the test case (e.g., electric regions and train routes) and the computational configurations (e.g., the estimated system efficiency). For a certain test case, comprehensive experiments could be done to correct the input parameters (e.g., the recuperation coefficient η for system efficiency) for increasing solution accuracy, and also to find the best option for making maximum use of the regenerated energy (e.g., locations of installing energy storage devices). We evaluate the performance indicators with regards to regenerative braking, including the storage rate of the regenerated energy, the utilization rate of the stored energy, the percentage of the energy loss due to system efficiency, and the reduction of the total energy consumption due to regenerative braking, shown in Fig. 7(a)-Fig. 7(d) respectively.

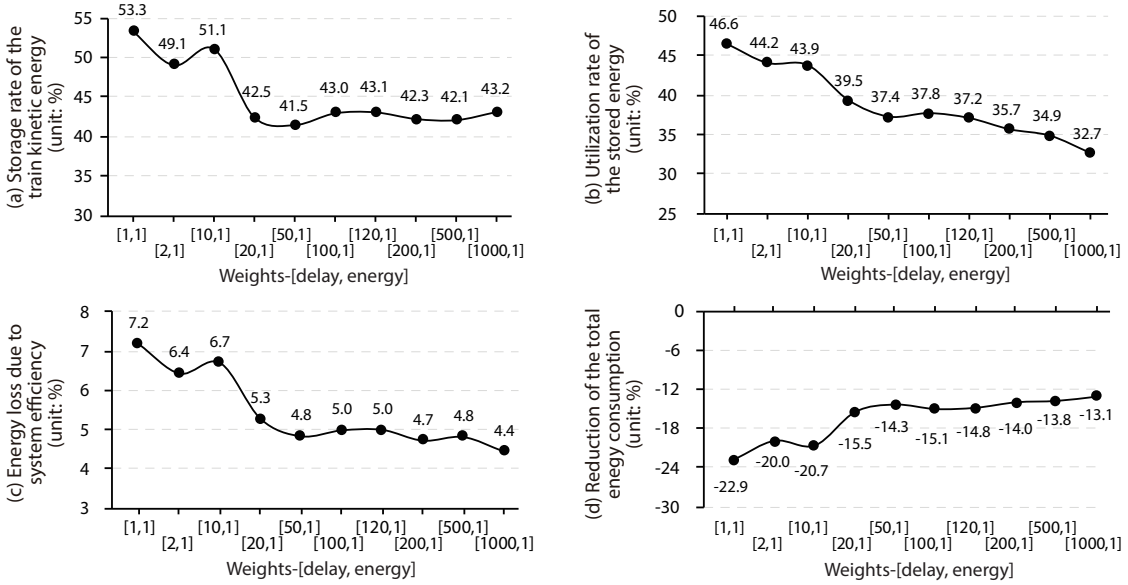

Figure 7. Storage rate of the train kinetic energy, utilization rate of the stored energy, energy loss due to system efficiency, and reduction of the total energy consumption

The results of the performance indicators differ for the different weights considered. Basically, an increase of the importance of the energy consumption leads to a larger storage rate of the train kinetic energy and a larger utilization rate of the regenerated energy; as a result, we obtain a larger reduction of the total energy consumption. The energy loss resulting from system efficiency also becomes larger with the increase of the storage rate and the utilization rate. In our case study, there is a surplus of the stored energy, i.e., not all of the stored energy are re-used for train acceleration; therefore, the reduction of the total energy consumption can increase even if the energy loss increases. Overall, based on the Dutch test case, 41.5%-53.3% of the train kinetic energy is stored in energy storage devices. About 4.4%-7.2% of this stored energy is lost due to system efficiency, and 32.7%-46.6% of this stored energy is re-utilized for train acceleration, which further leads to 13.1%-22.9% reduction of the total energy consumption. According to the experimental results, regenerative braking can significantly reduce the energy consumption of train operations, and it is an effective and practical way to achieve energy-efficient train operation. The results based on the Dutch test case show the effectiveness of the proposed formulations.

4.4. Comparison with the train speed profiles generated by a train trajectory optimization approach

In this section, we assess the results of the $\mathrm{P_{TSPO}}$ problem from a train control perspective. We adopt the nonlinear train speed profile optimization approach proposed by Wang et al. (2013) and apply the SQP approach to generate a speed profile for each train. The departure times at the origin and arrival times at the destinations of trains are given as time constraints for the train control problem. Moreover, the passing times at intermediate non-stopping stations and critical block sections are given as operational constraints, i.e., the traffic management problem is solved beforehand. For each train, a speed profile is generated with

the objective of minimizing the energy consumption. For the train control problem, each block section in the network is divided into 20 subsections and the acceleration or deceleration of trains is assumed to be a constant for each subsection. Since the SQP approach could result in local minima, we use 10 initial points for the calculation of the train speed profile for each train, and we select the best solution among the resulting speed profiles. The SQP approach uses a more accurate and refined model, so it can be seen as a more accurate approach for obtaining optimal speed profiles. We compare the train speed profiles generated by the P_{TSPO} approach and the SQP approach, as well as the resulting energy consumption. Note that we consider the P_{TSPO} approach with the weighted-sum formulation. As we aim at assessing the quality of the speed profiles generated by the P_{TSPO} problem, we do not consider the option of regenerative braking here for both the P_{TSPO} approach and the SQP approach.

Fig. 8 shows the speed-space trajectories obtained by the two approaches. For the sake of compactness, only one representative delay case with 15 trains is provided here. The train speed profiles of the P_{TSPO} solution and the SQP solution are indicated by solid lines and dashed lines respectively.

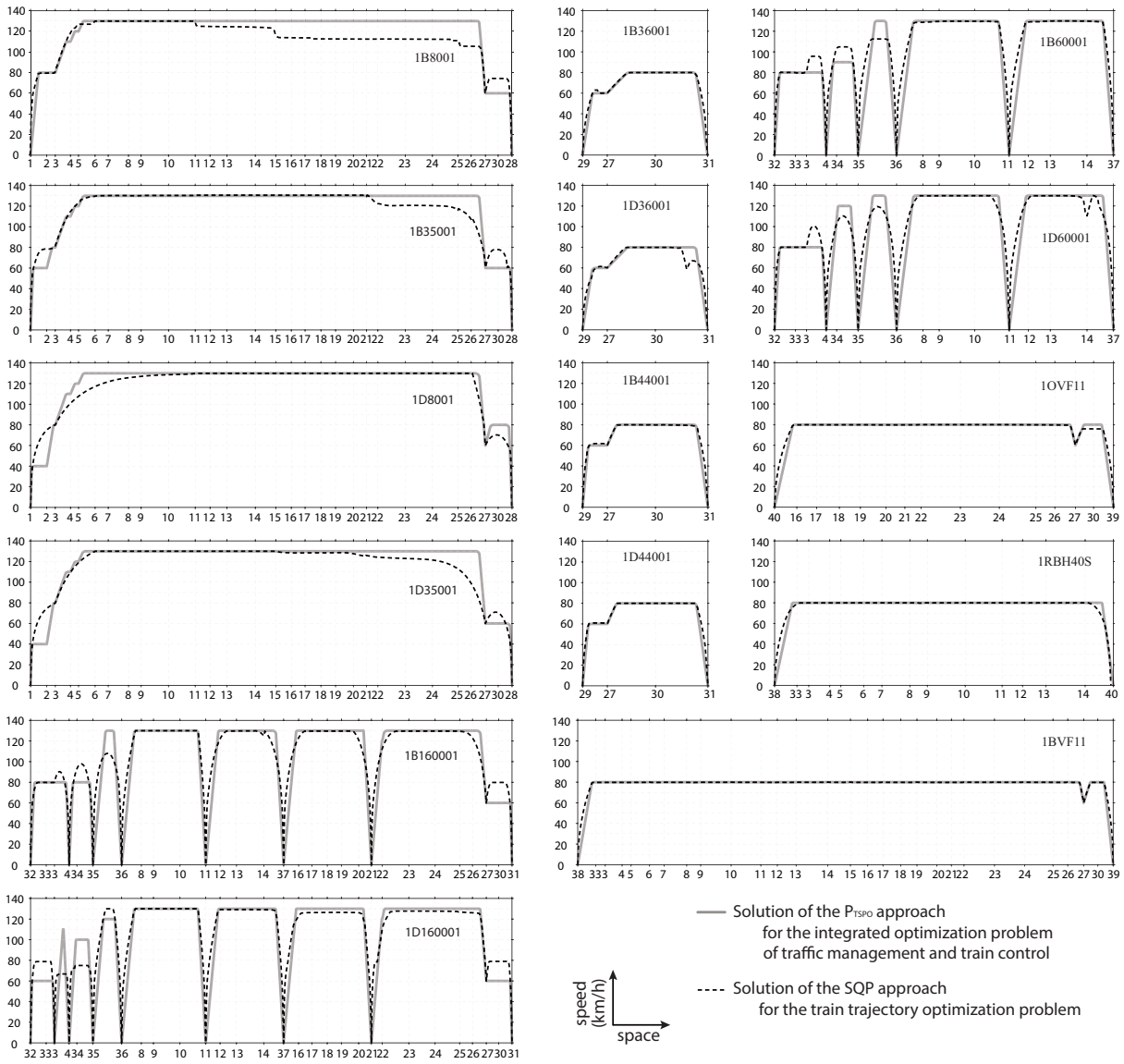

Figure 8. Comparison of the train speed profiles

It can be seen that the speed profiles generated by the SQP approach are smoother than those of the P_{TSPO} approach in acceleration and deceleration, as the SQP approach uses the detailed nonlinear train model. However, for most trains that travel sequentially on nodes $27 \rightarrow 30 \rightarrow 28$, the driving strategy obtained by the P_{TSPO} approach is more efficient for energy consumption. Due to the speed limit requirement for node 27, every train reduces its speed to 60 km/h while passing node 27. In the P_{TSPO} solution, most trains maintain a speed of 60 km/h after passing node 27 to further approach their destination, e.g., the 1B8001 and 1B16001 trains; a few trains accelerate to their maximum speeds after passing node 27, e.g., the 1D8001 train. In the SQP solution, every train that traverses node 27 accelerates after passing node 27 and then decelerates when approaching its destination. This may be caused by the different computational configurations of the two approaches and the sub-optimal solutions found by the two approaches. The train acceleration after passing node 27 needs to additionally use energy; therefore, the driving strategy of not accelerating the train after passing node 27, found by the P_{TSPO} approach, is more efficient in use of energy. For some trains, the speed profiles of the two approaches are highly coincident, e.g., the 1B36001 and 1BVF11 trains. The quality of the train speed profiles obtained by the P_{TSPO} approach is overall satisfactory, with regard to the solution found by the SQP approach.

In Fig. 9, we present the energy consumption of each train, computed by the P_{TSPO} approach (indicated in gray) and the SQP approach (indicated in black). The Y-axis indicates the energy consumption for each train, and the X-axis represents the train number.

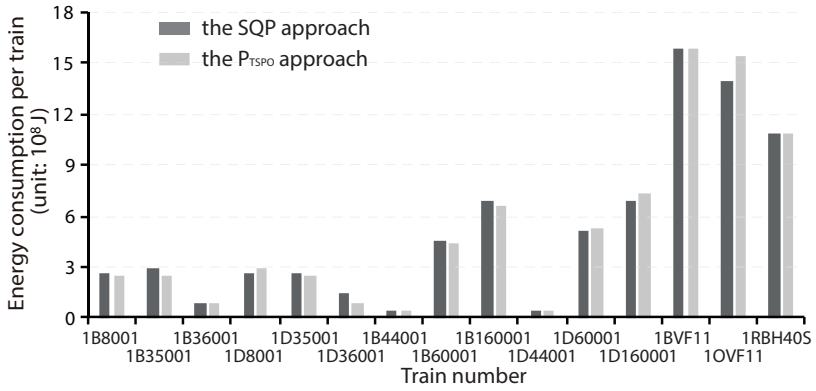

Figure 9. Comparison of the energy consumption for one representative delay case

When focusing on each single train, the energy consumption computed by the two approaches is different. For some trains, e.g., the 1B8001 and 1B35001 trains, the speed profiles found by the P_{TSPO} approach are better in efficient use of energy, mainly caused by the driving strategy of maintaining a speed of 60 km/h after passing node 27. For some other trains, e.g., the 1D160001 train, better speed profiles for energy efficiency are found by the SQP approach. However, the results of the total energy consumption of the two approaches are very close, i.e., 78.00×10^8(J) and 77.86×10^8(J) for the P_{TSPO} approach and the SQP approach respectively. The SQP approach overall performs better, as it finds better speed profiles in efficient use of energy; however, the relative difference of the total energy consumption obtained by the two approaches is very small, only 0.18%.

According to the comparison of the P_{TSPO} approach and the SQP approach, it is demonstrated that the control performance of the P_{TSPO} approach is good for both the quality of the speed profiles and the calculation of the energy consumption.

4.5. Summary of the experimental results

We here summarize the main conclusions, sketched quantitatively in Fig. 10 from the viewpoints of train delay (X-axis) and energy consumption (Y-axis), clarifying the trade-off between them. The experimental results reported in Sections 4.1-4.3 are all included in Fig. 10. Fig. 10(b) is a zoom-in of Fig. 10(a), with some

trend lines. We use symbols to distinguish the computation time limits considered for obtaining the solutions, i.e., the dot, square, plus, and cross symbols represent the initial solution, and the secondary solutions obtained within 180, 600, and 3600 seconds of computation time respectively. Each symbol indicates an average result of 10 delay cases, obtained within the given computation time limit. We use colors to indicate the multiple combined choices of the optimization approaches (i.e., the P_{NLP} and P_{TSPO} approaches), the formulation methods (i.e., the weighted-sum formulation and the ε-constraint formulation), and the option of regenerative braking. The blue and orange colors indicate the P_{NLP} solutions by using the weighted-sum formulation and the ε-constraint formulation respectively. The purple and gray colors indicate the P_{TSPO} solutions with the weighted-sum formulation and the ε-constraint formulation respectively. The green color represents the solution considering regenerative braking, obtained by the P_{TSPO} approach with the weighted-sum formulation.

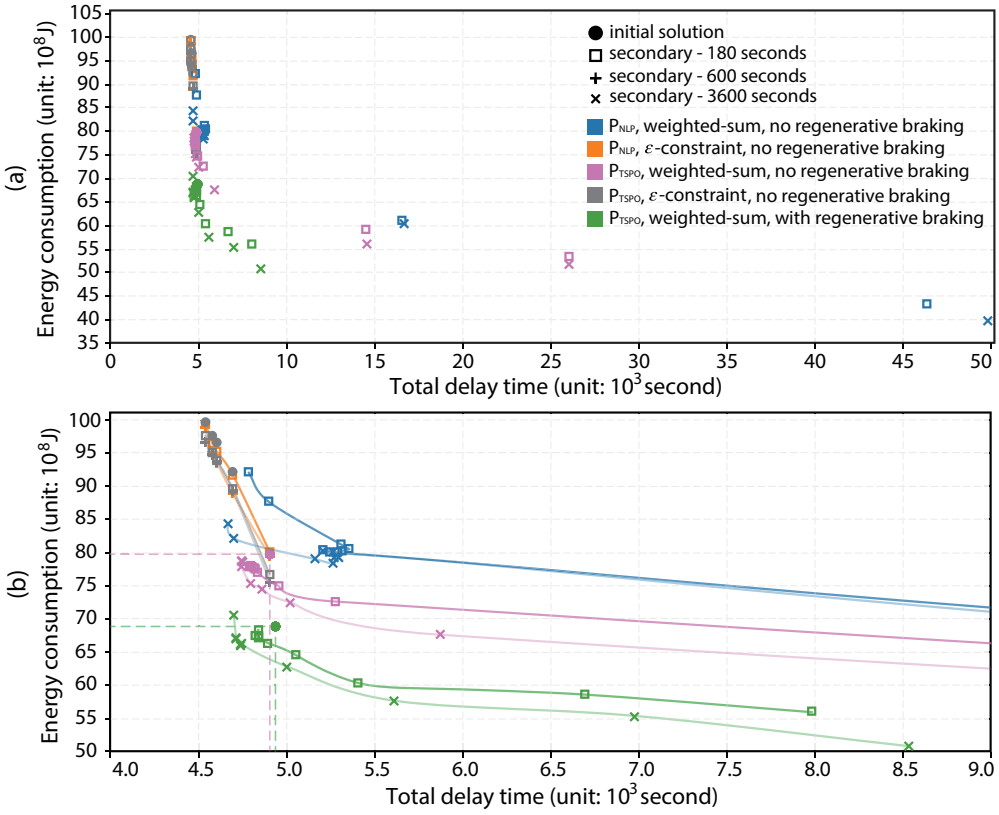

Figure 10. Overview of all experimental results, from the viewpoints of train delay and energy consumption

According to the experimental results presented in Section 4.1, the performance of the P_{TSPO} approach is better than the performance of the P_{NLP} approach. This is reflected in Fig. 10 by the lower purple line when comparing with the blue line in the case of using the weighted-sum formulation, and is also reflected by the gray line, which is mostly lower than the orange line when applying the ε-constraint formulation.

When using the ε-constraint formulation, the gray and orange trend lines in Fig. 10 go towards a larger energy consumption with a stricter upper bound on the train delay. Required as the input of the ε-constraint formulation, the upper bound for the train delay has to be carefully chosen; an inappropriate upper bound may lead to a bad performance on either train delay or energy consumption, and it may even cause infeasibility of the optimization problem. For the weighted-sum formulation, the results of the train delay and the energy consumption are widely ranged, depending on the weights considered, see the blue, purple, and green trend lines. Overall, for our case, the weighted-sum formulation is more applicable than

the ε-constraint formulation, as discussed in Section 4.2.

In Section 4.2.1, by using the $\mathrm{P_{TSPO}}$ approach with the weighted-sum formulation, we find better solutions, where the delay time and the energy consumption are reduced at the same time, compared with the initial solution that is obtained by considering a fixed full speed profile for each train on each block section. This is reflected by the symbols located between the purple dashed lines in Fig. 10; the vertical and horizontal dashed lines come from the initial solution (indicated by the purple dot symbol), given as benchmarks. Train delay and energy consumption can be improved simultaneously through managing the train speed, by up to 4.0% and 5.6% respectively. The simultaneous reduction of the two objectives also demonstrates the benefit of integrating traffic management and train control and shows great potential for energy efficiency of train operations.

When regenerative braking is applied, the total energy consumption for train operations is significantly reduced, indicated by the green lines in Fig. 10, which represent a smaller energy consumption in comparison with the purple lines. Applying regenerative braking is an effective way to achieve energy-efficient train operation (as discussed in Section 4.3).

The good quality of the train speed profiles generated by the $\mathrm{P_{TSPO}}$ approach is demonstrated in Section 4.4, compared with the train speed profiles obtained by the SQP approach, which is a more accurate approach for computing optimal speed profiles. The relative difference of the total energy consumption of the $\mathrm{P_{TSPO}}$ solution and the SQP solution is very small (only 0.18%), which also demonstrates the good control performance of the $\mathrm{P_{TSPO}}$ approach.

5. Conclusions and future research

In this paper (Part 2), we have considered extensions towards energy-efficient train operation, based on the integrated optimization approaches proposed in Part 1, where the traffic-related properties (i.e., departure times, arrival times, and train orders) and the train-related properties (i.e., train speed trajectory) are optimized simultaneously. We have first introduced energy evaluation into the integrated optimization approaches, calculating the energy used for train acceleration and the energy consumed for overcoming resistance. We have developed a set of linear constraints for the $\mathrm{P_{TSPO}}$ problem to compute the energy consumption. An approximation of the resistance function with a piecewise constant function has been applied for computing the energy consumption of the $\mathrm{P_{NLP}}$ and $\mathrm{P_{PWA}}$ problems. In addition, we have considered the option of regenerative braking and presented linear formulations to calculate the utilization of the energy obtained through regenerative braking. With the inclusion of the energy-related formulations, we could focus on two objectives, i.e., delay recovery and energy efficiency, by using the weighted-sum formulation and the ε-constraint formulation. Experiments have been conducted based on a real-world dataset adapted from the Dutch railway network (the same as Part 1). According to the experimental results, the $\mathrm{P_{TSPO}}$ approach overall performs better. Aiming at both delay recovery and energy efficiency, the two objectives can be improved at once (e.g., by up to 4.0% and 5.6% for the train delay and the energy consumption in one of the solutions) through managing the train speed. Moreover, for the test case, the application of regenerative braking leads to about 13.1%-22.9% reduction of the total energy consumption. By comparing with the train speed profiles obtained by the SQP approach, which is a more accurate approach for computing speed profiles, the good control performance of the $\mathrm{P_{TSPO}}$ approach has been demonstrated, as the speed profiles of the $\mathrm{P_{TSPO}}$ approach are similar to those obtained by the SQP approach.

In our future research, we will focus on developing distributed optimization methods and/or heuristic algorithms to improve the computational efficiency of the proposed optimization approaches and to increase their applicability to larger-scale networks. Based on the developments of computation efficient algorithms, a larger set of discrete speed values could be used to generate the possible TSPOs, in order to achieve an improvement in both accuracy and computational efficiency. Moreover, we can extend the proposed multi-objective optimization problem to consider some other relevant objectives, such as the cost of train operations and the passenger travel time. Finally, a decision support tool, embedded with the optimization approaches, could be developed, for both train dispatcher and train driver, in order to promote the research into reality.

Acknowledgments

This work is jointly supported by National Natural Science Foundation of China (71571012, 61503020, 61790573). The work of the first author is also supported by China Scholarship Council under Grant 201507090058.

References

Albrecht, A., Howlett, P., Pudney, P., Vu, X., Zhou, P., 2016a. The key principles of optimal train contro - part 1: Formulation of the model, strategies of optimal type, evolutionary lines, location of optimal switching points. Transportation Research Part B: Methodological 94, 482–508.

Albrecht, A., Howlett, P., Pudney, P., Vu, X., Zhou, P., 2016b. The key principles of optimal train contro - part 2: Existence of an optimal strategy, the local energy minimization principle, uniqueness, computational techniques. Transportation Research Part B: Methodological 94, 509–538.

Albrecht, A.R., Howlett, P.G., Pudney, P.J., Vu, X., 2013. Energy-efficient train control: from local convexity to global optimization and uniqueness. Automatica 49, 3072–3078.

Bemporad, A., Morari, M., 1999. Control of systems integrating logic, dynamics, and constraints. Automatica 35, 407–427.

Boizumeau, J., Leguay, P., Navarro, E., 2011. Braking energy recovery at the rennes metro, in: Proceedings of the Workshop on Braking Energy Recovery Systems–Ticket to Kyoto. Bielefeld, Germany.

Brünger, O., Dahlhaus, E., 2008. Railway Timetable & Traffic-Analysis, Modelling, Simulation (Chapter Running Time Estimation, pp. 58-82). Eurail Press.

Chang, C., Xu, D., 2000. Differential evolution based tuning of fuzzy automatic train operation for mass rapid transit system. Proceedings of the IEEE International Conference on Electric Power Applications 147, 206–212.

Chen, E., Yang, X., Ding, Y., 2014. An energy-efficient adjustment approach in subway systems, in: Proceedings of the 17th IEEE International Conference on Intelligent Transportation Systems (ITSC), IEEE. pp. 2774–2779.

Cheng, J., 1997. Analysis of optimal driving strategies for train control problems. Ph.D. thesis.

Cheng, J., Davydova, Y., Howlett, P., Pudney, P., 1999. Optimal driving strategies for a train journey with non-zero track gradient and speed limits. IMA Journal of Management Mathematics 10, 89–115.

Ciccarelli, F., Del Pizzo, A., Iannuzzi, D., 2014. Improvement of energy efficiency in light railway vehicles based on power management control of wayside lithium-ion capacitor storage. IEEE Transactions on Power Electronics 29, 275–286.

Cucala, A., Fernández, A., Sicre, C., Domínguez, M., 2012. Fuzzy optimal schedule of high speed train operation to minimize energy consumption with uncertain delays and driver's behavioral response. Engineering Applications of Artificial Intelligence 25, 1548–1557.

D'Ariano, A., Pranzo, M., Hansen, I.A., 2007. Conflict resolution and train speed coordination for solving real-time timetable perturbations. IEEE Transactions on Intelligent Transportation Systems 8, 208–222.

Davis, W.J., 1926. The tractive resistance of electric locomotives and cars. General Electric.

Franke, R., Meyer, M., Terwiesch, P., 2002. Optimal control of the driving of trains (optimale steuerung der fahrweise von zügen). Automatisierungstechnik 50, 606 – 614.

Garcia-Tabares, L., Iglesias, J., Lafoz, M., Martinez, J., Vazquez, C., Tobajas, C., Gomez-Alors, A., Echeandia, A., Lucas, J., Zuazo, C., et al., 2011. Development and testing of a 200 MJ/350 kW kinetic energy storage system for railways applications, in: Proceedings of the 9th World Congress on Railway Research, Lille, France, pp. 22–26.

Ghaviha, N., Campillo, J., Bohlin, M., Dahlquist, E., 2017. Review of application of energy storage devices in railway transportation. Energy Procedia 105, 4561–4568.

González-Gil, A., Palacin, R., Batty, P., 2013. Sustainable urban rail systems: Strategies and technologies for optimal management of regenerative braking energy. Energy Conversion and Management 75, 374–388.

González-Gil, A., Palacin, R., Batty, P., Powell, J., 2014. A systems approach to reduce urban rail energy consumption. Energy Conversion and Management 80, 509–524.

Haahr, J.T., Pisinger, D., Sabbaghian, M., 2017. A dynamic programming approach for optimizing train speed profiles with speed restrictions and passage points. Transportation Research Part B: Methodological 99, 167–182.

Han, S.H., Byen, Y.S., Baek, J.H., An, T.K., Lee, S.G., Park, H.J., 1999. An optimal automatic train operation (ato) control using genetic algorithms (ga), in: Proceedings of the IEEE Region 10 Conference (TENCON 99), IEEE, Cheju Island, South Korea. pp. 360–362.

Hansen, H.S., Nawaz, M.U., Olsson, N., 2017. Using operational data to estimate the running resistance of trains. estimation of the resistance in a set of norwegian tunnels. Journal of Rail Transport Planning & Management 7, 62–76.

Howlett, P., 1990. An optimal strategy for the control of a train. The ANZIAM Journal 31, 454–471.

Howlett, P., 2000. The optimal control of a train. Annals of Operations Research 98, 65–87.

Howlett, P.G., Pudney, P.J., 1995. Energy-Efficient Train Control. Springer.

Howlett, P.G., Pudney, P.J., Vu, X., 2009. Local energy minimization in optimal train control. Automatica 45, 2692–2698.

Huerlimann, D., Nash, A., 2003. Opentrack-simulation of railway networks, user manual version 1.3. ETH Zurich: Institute for Transportation Planning and Systems .

Ichikawa, K., 1968. Application of optimization theory for bounded state variable problems to the operation of train. Bulletin of JSME 11, 857–865.

Kampeerawat, W., Koseki, T., 2017. A strategy for utilization of regenerative energy in urban railway system by application of smart train scheduling and wayside energy storage system. Energy Procedia 138, 795–800.

Khaligh, A., Li, Z., 2010. Battery, ultracapacitor, fuel cell, and hybrid energy storage systems for electric, hybrid electric, fuel cell, and plug-in hybrid electric vehicles: State of the art. IEEE transactions on Vehicular Technology 59, 2806–2814.

Khmelnitsky, E., 2000. On an optimal control problem of train operation. IEEE Transactions on Automatic Control 45, 1257–1266.

Ko, H., Koseki, T., Miyatake, M., 2004. Application of dynamic programming to optimization of running profile of a train, in: Proceedings of Computers in Railways IX, WIT Press, Southhampton, Boston, MA, USA. pp. 103–112.

Kokotovic, P., Singh, G., 1972. Minimum-energy control of a traction motor. IEEE Transactions on Automatic control 17, 92–95.

Lambert, S., Pickert, V., Holden, J., He, X., Li, W., 2010. Comparison of supercapacitor and lithium-ion capacitor technologies for power electronics applications, in: Proceedings of 5th IET International Conference on Power Electronics, Machines and Drives (PEMD 2010), IET, Brighton, UK. p. 241.

Li, X., Lo, H.K., 2014. An energy-efficient scheduling and speed control approach for metro rail operations. Transportation Research Part B: Methodological 64, 73–89.

Liu, R.R., Golovitcher, I.M., 2003. Energy-efficient operation of rail vehicles. Transportation Research Part A: Policy and Practice 37, 917–932.

Lu, Q., Feng, X., 2011. Optimal control strategy for energy saving in trains under the four-aspect fixed autoblock system. Journal of Modern Transportation 19, 82–87.

Lu, S., 2011. Optimising power management strategies for railway traction systems. Ph.D. thesis. University of Birmingham.

Lüthi, M., 2009. Improving the efficiency of heavily used railway networks through integrated real-time rescheduling. Ph.D. thesis. ETH Zürich.

Mazzarello, M., Ottaviani, E., 2007. A traffic management system for real-time traffic optimisation in railways. Transportation Research Part B: Methodological 41, 246–274.

Meinert, M., 2009. New mobile energy storage system for rolling stock, in: Proceedings of the 13th European Conference on Power Electronics and Applications, IEEE. pp. 1–10.

Miyatake, M., Ko, H., 2010. Optimization of train speed profile for minimum energy consumption. IEEJ Transactions on Electrical and Electronic Engineering 5, 263–269.

Nasri, A., Moghadam, M.F., Mokhtari, H., 2010. Timetable optimization for maximum usage of regenerative energy of braking in electrical railway systems, in: Proceedings of the International Symposium on Power Electronics Electrical Drives Automation and Motion (SPEEDAM), IEEE. pp. 1218–1221.

Ogasa, M., 2010. Application of energy storage technologies for electric railway vehiclesexamples with hybrid electric railway vehicles. IEEJ Transactions on Electrical and Electronic Engineering 5, 304–311.

Peña-Alcaraz, M., Fernández, A., Cucala, A.P., Ramos, A., Pecharromán, R.R., 2012. Optimal underground timetable design based on power flow for maximizing the use of regenerative-braking energy. Proceedings of the Institution of Mechanical Engineers, Part F: Journal of Rail and Rapid Transit 226, 397–408.

Research Collection ETH Zurich, 2018. Detailed experimental results. https://www.research-collection.ethz.ch/handle/20.500.11850/256447.

Scheepmaker, G.M., Goverde, R.M., 2015. Running time supplements: energy-efficient train control versus robust timetables, in: Proceedings of the 6th International Conference on Railway Operations Modelling and Analysis (Rail-Tokyo 2015), Narashino, Japan, pp. 23–26.

Scheepmaker, G.M., Goverde, R.M., 2016. Energy-efficient train control including regenerative braking with catenary efficiency, in: Proceedings of the IEEE International Conference on Intelligent Rail Transportation (ICIRT), IEEE. pp. 116–122.

Scheepmaker, G.M., Goverde, R.M., Kroon, L.G., 2017. Review of energy-efficient train control and timetabling. European Journal of Operational Research 257, 355–376.

Shimada, M., Oishi, R., Araki, D., Nakamura, Y., 2010. Energy storage system for effective use of regenerative energy in electrified railways. Hitachi Review 59, 33–38.

Siemens, 2011. Increasing energy efficiency optimized traction power supply in mass transit systems. https://w3.usa.siemens.com/mobility/us/Documents/en/rail-solutions/railway-electrification/dc-traction-power-supply/increasing-energy-efficiency-en.pdf.

Steiner, M., Klohr, M., Pagiela, S., 2007. Energy storage system with ultracaps on board of railway vehicles, in: Proceedings of the European Conference on Power Electronics and Applications, IEEE. pp. 1–10.

Su, R., Gu, Q., Wen, T., 2014. Optimization of high-speed train control strategy for traction energy saving using an improved genetic algorithm. Journal of Applied Mathematics 2014.

Su, S., Li, X., Tang, T., Gao, Z., 2013. A subway train timetable optimization approach based on energy-efficient operation strategy. IEEE Transactions on Intelligent Transportation Systems 14, 883–893.

Su, S., Tang, T., Wang, Y., 2016. Evaluation of strategies to reducing traction energy consumption of metro systems using an optimal train control simulation model. Energies 9, 105.

UIC, 2002. Regenerative braking in DC systems. http://www.railway-energy.org/tfee/index.php?ID=220&TECHNOLOGYID=103&SEL=210&EXPANDALL=3.

UIC, 2012. Moving towards sustainable mobility: a strategy for 2030 and beyond for the European railway sector. http://www.cer.be/sites/default/files/publication/CER-UIC_Sustainable_Mobility_Strategy_-_SUMMARY.pdf.

Vardy, A., Reinke, P., 1999. Estimation of train resistance coefficients in tunnels from measurements during routine operation. Proceedings of the Institution of Mechanical Engineers, Part F: Journal of Rail and Rapid Transit 213, 71–87.

Vašak, M., Baotić, M., Perić, N., Bago, M., 2009. Optimal rail route energy management under constraints and fixed arrival time, in: Proceedings of the 2009 European Control Conference (ECC), pp. 2972–2977.

Wang, P., Goverde, R.M., 2016. Multiple-phase train trajectory optimization with signalling and operational constraints. Transportation Research Part C: Emerging Technologies 69, 255–275.

Wang, Y., De Schutter, B., van den Boom, T.J.J., Ning, B., 2012. Optimal trajectory planning for trains under operational constraints using mixed integer linear programming, in: Proceedings of the 13th IFAC Symposium on Control in Transportation Systems (CTS2012). Sofia, Bulgaria, pp. 158–163.

Wang, Y., De Schutter, B., van den Boom, T.J.J., Ning, B., 2013. Optimal trajectory planning for trains–a pseudospectral method and a mixed integer linear programming approach. Transportation Research Part C: Emerging Technologies 29, 97–114.

Wang, Y., De Schutter, B., van den Boom, T.J.J., Ning, B., 2014. Optimal trajectory planning for trains under fixed and moving signaling systems using mixed integer linear programming. Control Engineering Practice 22, 44–56.

Wang, Y., Ning, B., van den Boom, T.J.J., De Schutter, B., 2016. Optimal Trajectory Planning and Train Scheduling for Urban Rail Transit Systems. Springer.

Yang, S., Wu, J., Sun, H., Yang, X., Gao, Z., Chen, A., 2017a. Bi-objective nonlinear programming with minimum energy consumption and passenger waiting time for metro systems, based on the real-world smart-card data. Transportmetrica B: Transport Dynamics , 1–18.

Yang, S., Wu, J., Yang, X., Sun, H., Gao, Z., 2017b. Energy-efficient timetable and speed profile optimization with multi-phase speed limits: Theoretical analysis and application. Applied Mathematical Modelling 56, 32–50.

Yang, X., Chen, A., Li, X., Ning, B., Tang, T., 2015. An energy-efficient scheduling approach to improve the utilization of regenerative energy for metro systems. Transportation Research Part C: Emerging Technologies 57, 13–29.

Yang, X., Li, X., Gao, Z., Wang, H., Tang, T., 2013. A cooperative scheduling model for timetable optimization in subway systems. IEEE Transactions on Intelligent Transportation Systems 14, 438–447.

Appendix A Assumptions and formulation method introduced in Part 1

We recall the assumptions made in Part 1 as follows: (1) train acceleration is considered as a piecewise constant function by giving a fixed switching point (breakpoint) of speed (e.g., 60 km/h) for each train category; (2) train deceleration is constant for a certain train category and differs among train categories; (3) the speed limit is considered as constant for a certain train category on a certain block section, i.e., the minimum value of the designed train speed and the designed block section (track) speed, but differs among train categories and block sections; (4) the beginning/ending point of a block section or of a main/siding track in a station, or a point of merging/diverging of tracks on a segment, is represented by a node; (5) a block section is described as a cell, which connects two nodes in a pair; (6) a station is simplified to a number of main/siding track(s), which can be further modelled as a single cell or a set of cells; (7) for a double-track railway segment between two stations, each track is modelled as a sequence of directional cells (i.e., directional block sections), and for a single-track railway segment, the only track between two stations is modelled as bi-directional cells (i.e., bi-directional block section); (8) the speed of a train on a cell is divided into three phases, i.e., incoming, cruising, and outgoing phases, refer to Fig. 11, and train coasting is neglected (however, a coasting phase can be introduced by assuming a piecewise constant deceleration function of the cruising speed, as remarked in Section 3.3 of this paper); (9) only one train is allowed to access a cell at any time; (10) the time step (granularity of time) is one second.

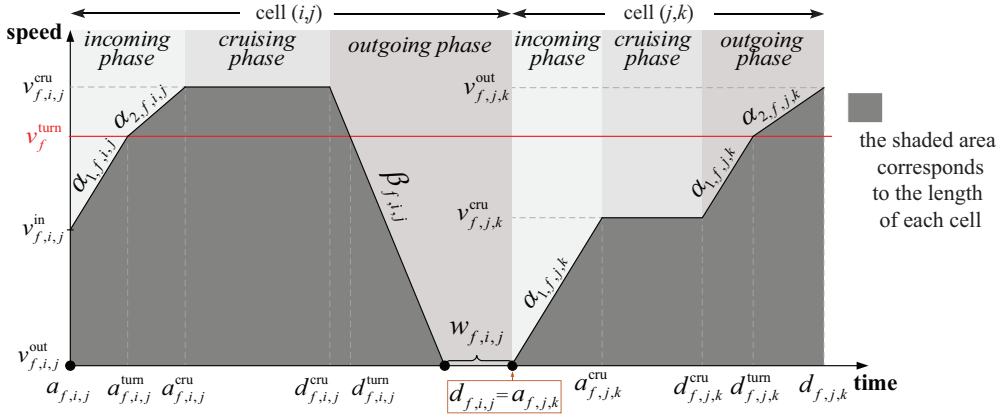

Figure 11. Speed-time graph of train f on cell (i, j) and cell (j, k) to illustrate the relevant decision variables

We recall and briefly explain the formulation method proposed in Part 1. The trajectory of each train on each cell is divided into three phases: incoming, cruising, and outgoing phases, as illustrated in Fig. 11, where train f enters cell (i, j) at time $a_{f,i,j}$ with a speed $v^{\text{in}}_{f,i,j}$, and then a sequence of the following actions is taken on cell (i, j):

1) in the time interval $[a_{f,i,j}, a^{\text{turn}}_{f,i,j}]$, the train accelerates from speed $v^{\text{in}}_{f,i,j}$ to speed v^{turn}_{f} at a steady acceleration $\alpha_{1,f,i,j}$;
2) in the time interval $[a^{\text{turn}}_{f,i,j}, a^{\text{cru}}_{f,i,j}]$, the train accelerates from speed v^{turn}_{f} to speed $v^{\text{cru}}_{f,i,j}$ at a steady acceleration $\alpha_{2,f,i,j}$;
3) in the time interval $[a^{\text{cru}}_{f,i,j}, d^{\text{cru}}_{f,i,j}]$, the train keeps a constant speed $v^{\text{cru}}_{f,i,j}$;
4) in the time interval $[d^{\text{cru}}_{f,i,j}, d_{f,i,j} - w_{f,i,j}]$, the train decelerates from speed $v^{\text{cru}}_{f,i,j}$ to speed $v^{\text{out}}_{f,i,j}$ (i.e., 0 km/h in this case) at a steady deceleration $-\beta_{f,i,j}$;
5) in the time interval $[d_{f,i,j} - w_{f,i,j}, d_{f,i,j}]$, the train dwells in cell (i,j).

Then, train f departs from cell (i,j) at time $d_{f,i,j}$. Meanwhile, train f arrives at cell (j,k) at time $a_{f,j,k}$, and starts accelerating. As train f does not reach the switching speed v^{turn}_{f} in the incoming phase of cell (j,k), only one acceleration $\alpha_{1,f,i,j}$ is used. Note that the sequence of the action(s) taken by a train on a cell do not follow a pre-specified frame (like the one described above); in fact, it is determined by optimizing the time variables (a/d) and speed variables (v). For instance, a train may take a sequence of actions to first accelerate and then decelerate on a cell (i.e., $v^{\text{in}}_{f,i,j} < v^{\text{cru}}_{f,i,j}$ and $v^{\text{out}}_{f,i,j} < v^{\text{cru}}_{f,i,j}$), and it may also take only one action to keep a constant speed traversing the cell (i.e., $v^{\text{in}}_{f,i,j} = v^{\text{cru}}_{f,i,j} = v^{\text{out}}_{f,i,j}$).

Table 2. Explanation of the speed indicators $\zeta_{1,f,i,j,b}, ..., \zeta_{6,f,i,j,b}$ for train f on cell (i,j), used in the P_{TSPO} optimization approach

	Incoming phase			Outgoing phase		
Speed conditions	$y^{\text{in}}_{f,i,j,b} \le y^{\text{cru}}_{f,i,j,b}$	$v^{\text{turn}}_{f} \le y^{\text{in}}_{f,i,j,b}$	$y^{\text{cru}}_{f,i,j,b} \le v^{\text{turn}}_{f}$	$y^{\text{cru}}_{f,i,j,b} \le y^{\text{out}}_{f,i,j,b}$	$v^{\text{turn}}_{f} \le y^{\text{cru}}_{f,i,j,b}$	$y^{\text{out}}_{f,i,j,b} \le v^{\text{turn}}_{f}$
	$\Updownarrow$	$\Updownarrow$	$\Updownarrow$	$\Updownarrow$	$\Updownarrow$	$\Updownarrow$
Speed indicators	$\zeta_{1,f,i,j,b} = 1$	$\zeta_{3,f,i,j,b} = 1$	$\zeta_{4,f,i,j,b} = 1$	$\zeta_{2,f,i,j,b} = 1$	$\zeta_{5,f,i,j,b} = 1$	$\zeta_{6,f,i,j,b} = 1$

To formulate the uniformly accelerating and decelerating motions, six logical speed indicators $\zeta_{1,f,i,j,b}$, ..., $\zeta_{6,f,i,j,b}$ are used to indicate the train speeds in the speed profile vector $y_{f,i,j,b}$. Table 2 gives an overview of the link between the speed conditions and the speed indicators for the incoming and outgoing phases. These speed indicators are used to compute the energy $J^{\text{res\_in}}_{f,i,j}$, $J^{\text{res\_cru}}_{f,i,j}$, and $J^{\text{res\_out}}_{f,i,j}$ consumed to overcome resistance in the incoming, cruising, and outgoing phases for the P_{TSPO} approach, formulated as (20)-(21) in Section 3.2.2.

Appendix B Additional explanations of the formulations in Section 3

In previous studies on the train control problem (Wang et al. 2013, Wang and Goverde 2016), the energy used for a train that travels from position x_1 to position x_2 is calculated by using the following equation:

$$J = \int_{x_1}^{x_2} q(x) \cdot \mathrm{d}x = \int_{x_1}^{x_2} m \cdot \alpha \cdot \mathrm{d}x + \int_{x_1}^{x_2} r^{\text{x}}(x) \cdot \mathrm{d}x, \tag{16}$$

where J indicates the work (energy consumption), $q(\cdot)$ and $r^{\text{x}}(\cdot)$ indicate the tractive force and resistance force respectively, given as a function of the distance x, m is the train mass, and α indicates the train acceleration. By using the formulas $\mathrm{d}x = v \cdot \mathrm{d}t$ and $\mathrm{d}v = \alpha \cdot \mathrm{d}t$, we can rewrite (16) as follows:

$$J = \int_{v_1}^{v_2} m \cdot v \cdot \mathrm{d}v + \int_{v_1}^{v_2} \frac{r(v) \cdot v}{\alpha} \cdot \mathrm{d}v, \tag{17}$$

where the resistance force $r(\cdot)$ is given as a function of the train speed v, and v_1 and v_2 indicate the train speeds at the positions x_1 and x_2 respectively. The first term of (17) in fact indicates the energy used for accelerating trains, and the second term calculates the energy consumption for overcoming resistance.

With integral calculation, the energy consumption for train acceleration, i.e., the first term of (17), can be easily calculated as $\frac{m}{2} \cdot (v_2^2 - v_1^2)$, which is in fact the difference of the train kinetic energy when changing the train speed from v_1 to v_2 and applied in (1)-(2) of Section 3.2.1.

The second term of (17) is used to describe the energy consumed for overcoming resistance in Section 3.2.2. We next explain and derive the formulations for calculating the energy used for overcoming resistance. First, we need to construct a resistance function $r(\cdot)$, which typically includes two categories in the train motion, i.e., the train resistance and the line resistance.

The train resistance $r^{\text{train}}(\cdot)$ is the resistance that operates on the train because of movement, including roll resistance and air resistance, and it is generally considered as a function of the train speed v in the following form (Davis 1926, Brünger and Dahlhaus 2008):

$$r^{\text{train}}(v) = m \cdot g^{\text{grav}} \cdot (r_1 \cdot v^2 + r_2 \cdot v + r_3), \tag{18}$$

with the gravitational acceleration g^{grav} and non-negative coefficients $r_\varrho \geq 0$, $\varrho \in \{1, 2, 3\}$, which depend on the train characteristics.

The line resistance $r^{\text{line}}(\cdot)$ is the resistance caused by track grade, curves, and tunnels. According to Wang et al. (2013) and Hansen et al. (2017), the line resistance $r^{\text{line}}(\cdot)$ can be described by

$$\begin{aligned} &r^{\text{line}}(x, v) = r^{\text{grade}}(\lambda_x) + r^{\text{curve}}(\phi_x) + r^{\text{tunnel}}(l_x, v), \\ &\text{with} \begin{cases} r^{\text{grade}}(\lambda_x) = m \cdot g^{\text{grav}} \cdot \sin(\lambda_x), \\ r^{\text{curve}}(\phi_x) = m \cdot g^{\text{grav}} \cdot \frac{C^{\text{curve}}(\phi_x)}{\phi_x}, \\ r^{\text{tunnel}}(l_x, v) = m \cdot g^{\text{grav}} \cdot C^{\text{tunnel}}(l_x) \cdot v^2, \end{cases} \end{aligned} \tag{19}$$

where λ_x, ϕ_x, and l_x are the slope, curve radius, and the tunnel length along the track respectively, $C^{\text{curve}}(\cdot)$ is a coefficient that depends on the curve radius, and $C^{\text{tunnel}}(\cdot)$ is a coefficient that depends on many factors, e.g., the tunnel length.

In the literature on train optimal control, the curve resistance and the tunnel resistance are often ignored in calculations (which is concluded in the recent survey of Scheepmaker et al. 2017). The curve resistance, which is the result of the flange of the wheel hitting the rail and thereby increasing resistance, is relatively low compared to the grade resistance and therefore often ignored (Brünger and Dahlhaus 2008). Tunnel resistances are also often ignored because of the lack of general formulas that describe this resistance (Scheepmaker and Goverde 2015). When taking them into account, the curve resistance $r^{\text{curve}}(\cdot)$ and the tunnel resistance $r^{\text{tunnel}}(\cdot)$ in (19) are commonly given by empirical formulas. An example of such an empirical formula of the curve resistance is Roeckl's formula (Huerlimann and Nash 2003); for the tunnel resistance, an empirical formula is given by Vardy and Reinke (1999).

Based on the above formulas to calculate the different resistances, the total resistance force $r(\cdot)$ in a train motion can be expressed as a quadratic function of the speed, i.e., $r(x, v) = r^{\text{train}}(v) + r^{\text{line}}(x, v) = r_{1,x} \cdot v^2 + r_{2,x} \cdot v + r_{3,x}$, which is also applied in Section 3.2.2 to formulate the energy consumption for overcoming resistance.

For the P_{TSPO} problem, we can reformulate (3) and (4) as follows:

$$\begin{aligned} J^{\text{res\_in}}_{f,i,j} = &\sum_{b=1}^{|Y_{f,i,j}|} \vartheta_{f,i,j,b} \cdot \zeta_{1,f,i,j,b} \cdot \zeta_{4,f,i,j,b} \cdot \tfrac{\Xi_{f,i,j}(y^{\text{cru}}_{f,i,j,b}) - \Xi_{f,i,j}(y^{\text{in}}_{f,i,j,b})}{\alpha_{1,f,i,j}} \\ &+ \sum_{b=1}^{|Y_{f,i,j}|} \vartheta_{f,i,j,b} \cdot \zeta_{1,f,i,j,b} \cdot \zeta_{3,f,i,j,b} \cdot \tfrac{\Xi_{f,i,j}(y^{\text{cru}}_{f,i,j,b}) - \Xi_{f,i,j}(y^{\text{in}}_{f,i,j,b})}{\alpha_{2,f,i,j}} \\ &+ \sum_{b=1}^{|Y_{f,i,j}|} \vartheta_{f,i,j,b} \cdot \zeta_{1,f,i,j,b} \cdot (1 - \zeta_{3,f,i,j,b}) \cdot (1 - \zeta_{4,f,i,j,b}) \\ &\qquad \cdot \left[\tfrac{\Xi_{f,i,j}(v^{\text{turn}}_f) - \Xi_{f,i,j}(y^{\text{in}}_{f,i,j})}{\alpha_{1,f,i,j}} + \tfrac{\Xi_{f,i,j}(y^{\text{cru}}_{f,i,j}) - \Xi_{f,i,j}(v^{\text{turn}}_f)}{\alpha_{2,f,i,j}} \right] \end{aligned} \quad \forall f \in F, (i,j) \in E_f. \tag{20}$$

$$J^{\text{res\_cru}}_{f,i,j} = \sum_{b=1}^{|Y_{f,i,j}|} \vartheta_{f,i,j,b} \cdot \left(L^{\text{cell}}_{i,j} - L^{\text{in}}_{f,i,j,b} - L^{\text{out}}_{f,i,j,b} \right) \cdot \left(r_{1,f,i,j} \cdot {y^{\text{cru}}_{f,i,j,b}}^2 + r_{2,f,i,j} \cdot y^{\text{cru}}_{f,i,j,b} + r_{3,f,i,j} \right), \forall f \in F, (i,j) \in E_f. \tag{21}$$

The binary variable $\vartheta_{f,i,j,b}$ and the input parameters $y^{\text{in}}_{f,i,j,b}$, $y^{\text{cru}}_{f,i,j,b}$, $y^{\text{out}}_{f,i,j,b}$, $L^{\text{cell}}_{i,j}$, etc. have all been introduced in Part 1, and they are recalled in Table 1. The speed indicators $\zeta_{1,f,i,j,b}$, ..., $\zeta_{6,f,i,j,b}$ are used in Part 1 and explained in Table 2 of Appendix A. A formulation similar to (20) can also be constructed for calculating the energy consumption $J^{\text{res\_out}}_{f,i,j}$ in the outgoing phase; we skip the details here for the sake of compactness. With the inclusion of (20) and (21), the nature of the P_{TSPO} problem will not change.

As discussed in Section 3, we can approximate the resistance function $r_{f,i,j}(\cdot)$ by using a piecewise

constant function with 2 affine parts and with constant values $r^{\text{cs}}_{1,f,i,j}$ and $r^{\text{cs}}_{2,f,i,j}$, for the P_{NLP} problem and the P_{PWA} problem, in order to address the solving difficulties. As a result, we can use the following formulations to calculate the energy used by train f on cell (i,j) for overcoming resistance in the incoming and cruising phases respectively:

$$J^{\text{res\_in}}_{f,i,j} = \begin{cases} \frac{r^{\text{cs}}_{1,f,i,j}}{2\alpha_{1,f,i,j}} \cdot \left[(v^{\text{cru}}_{f,i,j})^2 - (v^{\text{in}}_{f,i,j})^2\right], \text{ if } v^{\text{in}}_{f,i,j} \le v^{\text{cru}}_{f,i,j} \le v^{\text{turn}}_{f} \\ \frac{r^{\text{cs}}_{2,f,i,j}}{2\alpha_{2,f,i,j}} \cdot \left[(v^{\text{cru}}_{f,i,j})^2 - (v^{\text{in}}_{f,i,j})^2\right], \text{ if } v^{\text{turn}}_{f} \le v^{\text{in}}_{f,i,j} < v^{\text{cru}}_{f,i,j} \\ \frac{r^{\text{cs}}_{1,f,i,j}}{2\alpha_{1,f,i,j}} \cdot \left[(v^{\text{turn}}_{f,i,j})^2 - (v^{\text{in}}_{f,i,j})^2\right] + \frac{r^{\text{cs}}_{2,f,i,j}}{2\alpha_{2,f,i,j}} \cdot \left[(v^{\text{cru}}_{f,i,j})^2 - (v^{\text{turn}}_{f,i,j})^2\right], \\ \qquad\qquad \text{if } v^{\text{in}}_{f,i,j} < v^{\text{turn}}_{f} < v^{\text{cru}}_{f,i,j} \\ 0, \quad \text{if } v^{\text{in}}_{f,i,j} > v^{\text{cru}}_{f,i,j} \end{cases} \quad \forall f \in F, (i,j) \in E_f \tag{22}$$

$$J^{\text{res\_cru}}_{f,i,j} = \begin{cases} r^{\text{cs}}_{1,f,i,j} \cdot L^{\text{cru}}_{f,i,j}, & \text{if } v^{\text{cru}}_{f,i,j} \le v^{\text{turn}}_{f} \\ r^{\text{cs}}_{2,f,i,j} \cdot L^{\text{cru}}_{f,i,j}, & \text{if } v^{\text{cru}}_{f,i,j} > v^{\text{turn}}_{f} \end{cases}, \quad \forall f \in F, (i,j) \in E_f. \tag{23}$$

These two equations derive from the work formula $J = r \cdot x$, where J and r indicate the energy consumption and the resistance force and $x = \frac{v_2^2 - v_1^2}{2\alpha}$ computes the distance travelled by a train for accelerating from speed v_1 to v_2 in a uniform acceleration motion. A formulation similar to (22) can also be constructed for calculating the energy consumption $J^{\text{res\_out}}_{f,i,j}$ in the outgoing phase. For the sake of compactness, we do not report those details here.